



HAL
open science

Palladium-Catalyzed Electrophilic C-H-Bond Fluorination: Mechanistic Overview and Supporting Evidence

Christelle Testa, Julien Roger, Paul Fleurat-Lessard, Jean-Cyrille Hierso

► **To cite this version:**

Christelle Testa, Julien Roger, Paul Fleurat-Lessard, Jean-Cyrille Hierso. Palladium-Catalyzed Electrophilic C-H-Bond Fluorination: Mechanistic Overview and Supporting Evidence. *European Journal of Organic Chemistry*, 2019, Organic Reaction Mechanisms, 2019 (2-3), pp.233-253. 10.1002/ejoc.201801138 . hal-03481415

HAL Id: hal-03481415

<https://hal.science/hal-03481415v1>

Submitted on 15 Dec 2021

HAL is a multi-disciplinary open access archive for the deposit and dissemination of scientific research documents, whether they are published or not. The documents may come from teaching and research institutions in France or abroad, or from public or private research centers.

L'archive ouverte pluridisciplinaire **HAL**, est destinée au dépôt et à la diffusion de documents scientifiques de niveau recherche, publiés ou non, émanant des établissements d'enseignement et de recherche français ou étrangers, des laboratoires publics ou privés.

Palladium-Catalyzed C–H Bond Electrophilic Fluorination: Mechanistic Overview and Supporting Evidences

Christelle Testa,^[a] Julien Roger,^{*[a]} Paul Fleurat-Lessard,^{*[a]} and Jean-Cyrille Hierso^{*[a, b]}

Abstract: Palladium-catalyzed electrophilic fluorination is a particularly attractive and challenging synthetic issue. Because of the rapid evolution of this topic, a critical point on the mechanistic and experimental advances is provided herein. In the present review we focused at current mechanistic understanding in electrophilic fluorination (and related halogenations) catalyzed by palladium, mainly with *N*-directing group. Our discussion is based on the well-characterized or calculated pertinent metal species and intermediates used for analyzing the plausible catalytic cycles. A particular effort has

been devoted to gather supporting data for the putative species involved in catalysis, such as mass data, NMR in solution (¹⁹F, ³¹P) and X-Ray structures, often supported by theoretical approaches. The cut-off of this review is March 2018.

1. Introduction

Synthetic application of halide compounds is a major driving force in the development of current organic chemistry. Organic halides encountered in Nature are formed through enzymatic metabolic routes,¹ photochemical reactions,² and geothermal events.³ Manmade halogenated aromatic and aliphatic compounds originally resulted from addition and substitution reaction approaches that became cornerstones of synthetic organic chemistry. The emergence of transition metal-promoted reactions allowed much progress in carbon–halogen bond chemistry.^{4,5,6,7,8} Selective and efficient metal catalysis served at breaking carbon–halogen bonds towards straightforward carbon atom functionalization, and was also used to form C–X bonds (X = F, Cl, Br, I). The direct functionalization of inert C–H bonds appeared particularly appealing. Efficient functionalization of typically strong and kinetically inert C–H bonds benefited from transition-metal C–H bond activation, and the use of a directing group allowed to overcome potential issues in the selectivity control. Consequently, transition metal catalyzed C–H bond halogenation for C–X bond formation experienced significant development and increasing efficiency. Relevant reviews concerning general palladium-catalyzed C–H activation/functionalization and halogenation (including fluorination) are available with relevant complementary perspectives.^{9,10,11,12,13,14} Because of the rapid evolution of this topic, a point on the mechanistic and experimental advances appeared to us desirable. In the present review we focused at current mechanistic understanding in palladium-catalyzed *N*-ligand-directed palladium-catalyzed C–H bond electrophilic fluorination. Our discussion is based on the well-characterized or calculated pertinent metal species and intermediates used for analyzing the plausible catalytic cycles. Herein, a particular effort

has been devoted to gather supporting data for the putative species involved in catalysis, such as mass data, NMR in solution and X-Ray structures, often supported by theoretical approaches by DFT. In particular, ¹⁹F NMR data are accurately reported related to palladium species and geometries involved. Palladium-catalyzed electrophilic fluorination is a particularly challenging synthetic issue, and we found sometimes appropriate to illustrate also a selection of related palladium-catalyzed functionalization, especially concerning halogenation reactions (typically chlorination, bromination and iodination). In this context, we also discussed herein recent synthetic advances in palladium-catalyzed fluorination with various organics, such as for instance some unusual directing groups like highly functionalized pyrazoles, electron-poor tetrazines, or chiral transient groups.

Christelle Testa studied chemistry in the Claude Bernard University at Lyon (2013 MSc degree). She obtained her PhD degree in chemistry in 2016 from the Université de Bourgogne Franche-Comté (UBFC) under the supervision of J.-C. Hierso and J. Roger. Her research interest are focused on the development of new methodologies in palladium-catalyzed C–H bond activation for halogenation.



Julien Roger received his PhD in chemistry at the Université de Rennes I in 2010 under the supervision of H. Doucet, working on palladium-catalyzed C–H arylation of heteroaromatic compounds. He joined the group of S. Yamaguchi at Nagoya University as a JSPS fellow, working on the synthesis of materials based on main group elements. In 2013, he joined the group of J.-C. Hierso as a Maître de Conférences. His current research focuses on transition metals C–H activation (Pd, Ru) for C–heteroatom bond formation, and related mechanistic understanding.



Paul Fleurat-Lessard studied at the ENS-Paris and obtained his PhD working with F. Volatron at the Université Paris-Sud Orsay. He worked as postdoctoral research associate in the groups of R. Schinke (Göttingen, Germany) and T. Ziegler



[a] Dr. C. Testa, Dr. J. Roger, Prof. Dr. P. Fleurat-Lessard, Prof. Dr. J.-C. Hierso
Institut de Chimie Moléculaire de l'Université de Bourgogne, UMR-CNRS 6302 – Université de Bourgogne Franche-Comté
9, avenue Alain Savary 21078 Dijon (France)
E-mail: julien.roger@u-bourgogne.fr; paul.fleurat-lessard@u-bourgogne.fr; jean-cyrille.hierso@u-bourgogne.fr

[b] Institut Universitaire de France (IUF), 103 Boulevard Saint Michel, 75005 Paris Cedex (France)

MICROREVIEW

(Calgary, Canada). In 2003, he was appointed Maître de Conférences at the ENS-Lyon, and was promoted Full Professor in 2015 at the Université de Bourgogne Franche Comté (UBFC). His research program is based on developing and applying theoretical tools to study mechanisms of organic and organometallic reactions.

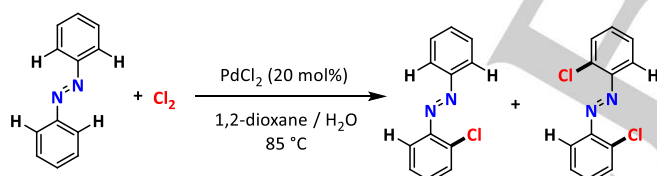
Jean-Cyrille Hiero has been Full Professor of Chemistry since 2009 and is now Deputy Director of the Institute of Molecular Chemistry (ICMUB, UMR-CNRS 6302, Dijon-France) at the Université de Bourgogne Franche Comté (UBFC) after having headed for six years the department of "Organometallic and Catalysis" (OCS) at the Institute of Molecular Chemistry. He has research interest in the fields of organometallic chemistry, ligand design, hetero- and homogeneous catalysis, chemical physics, and nano- and material sciences. He was awarded an *Institut Universitaire de France* (IUF) membership by the end of 2012.



2. Mechanistic advances in C–F bond formation involving Pd(II)/Pd(IV) species

2.1. Pioneering works in Pd-catalyzed C–H halogenation

Fahey early on in the seventies reported that palladium dichloride could be used in C–H chlorination catalysis of 1,2-diphenyldiazene with Cl₂, albeit giving a mixture of variously chlorinated products in low yields because of the four possible *ortho*-C–H bonds accessible from a *N*-directed process (Scheme 1).¹⁵



Scheme 1. 1,2-diphenyldiazene palladium-catalyzed *N*-directed *ortho*-C–H chlorination.

However, it is only in the last decade that the mechanistic studies of *ortho*-directed palladium-catalyzed C–X coupling reactions (with X = F, Cl, Br, I) have really started to be addressed. The palladium (IV) putative intermediates are generally rather unstable, and the iodinated palladium (IV) complex **a1**, *fac*-trimethyl (2,2'-bipyridyl)iodopalladium(IV), has been isolated and characterized only in 1986 by Canty *et al.* (Figure 1, oxidative addition of iodomethane to dimethyl(2,2'-bipyridyl)palladium(II) in acetone provided **a1**).¹⁶

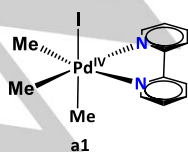
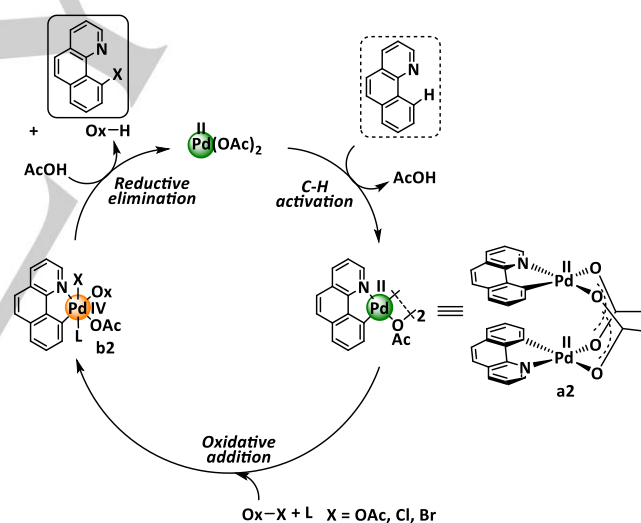


Figure 1. *fac*-trimethyl(2,2'-bipyridyl)iodopalladium(IV).

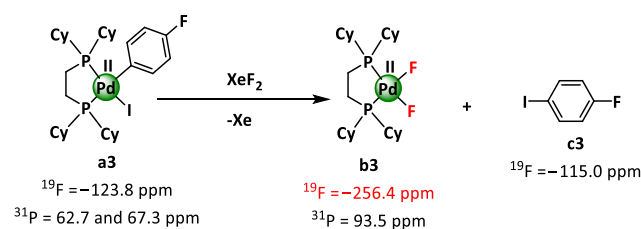
Based on the works of Fahey,¹⁵ Henry,¹⁷ Stock,¹⁸ and Crabtree,¹⁹ in 2004, the Sanford group described a general Pd(II)/Pd(IV) mechanism for the C–O,²⁰ then C–C,²¹ and C–X²² (X = Cl, Br, F) bond formation from *N*-directed ligand *ortho*-C–H activation (Scheme 2).^{10b} In the presence of one equivalent of Pd(OAc)₂, benzo[*h*]quinoline coordinates palladium to form a dinuclear complex bridged by acetate ligands. Then, after adding a strong oxidant, the palladium complex undergoes an oxidative addition, forming a new Pd(IV) species. Subsequent reductive elimination (RE) allows the formation of a C–X bond (X = O, Cl, Br) and the release of a palladium (II) complex.

2.2. Palladium-mediated C–F bond formation from Pd(II)

Following these seminal works on Pd-catalyzed C–H *ortho*-functionalization devoted mainly at C–X coupling with X = O, Cl, Br, several groups focused at the mechanism of related fluorination reaction.²³ The Vigalok group studied the formation of palladium(II) and palladium(IV) complexes incorporating fluorine atoms.²⁴ Vigalok *et al.* investigated the reactivity of xenon difluoride (XeF₂) to palladium (II) complexes (Scheme 3). The aryl iodide Pd(II) complex **a3**, which is stabilized by a chelating alkylbisphosphine, react with XeF₂ to give the palladium (II) difluoride complex **b3** (Scheme 3) via a phenyl iodide reductive elimination process. The complex **b3** is characterized in particular by a ¹⁹F NMR signal at –256.0 ppm for the two fluorides in *trans* position to phosphorus atoms.²⁵

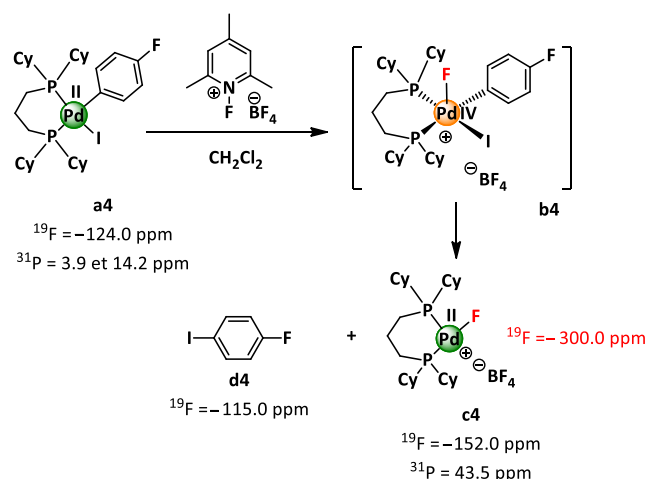


Scheme 2. General mechanistic view of C–H bond functionalization.



Scheme 3. Pd(II) difluoride synthesis from XeF₂.

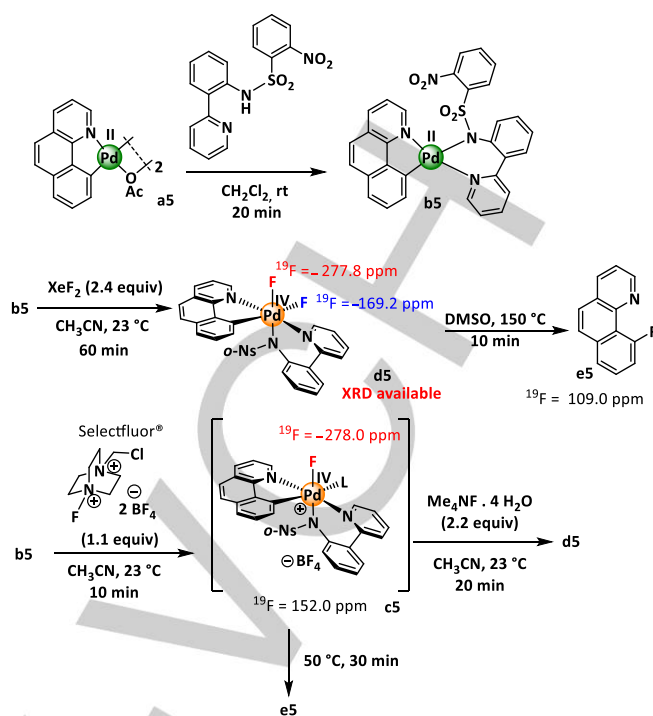
They also investigated the reactivity of *N*-fluoro-2,4,6-trimethylpyridinium tetrafluoroborate on the same kind of palladium(II) complex (**a4**, Scheme 4) to achieve the formation of a cationic Pd(II) fluoride **c4**.



Scheme 4. Pd(II) fluoride synthesis from *N*-fluoropyridinium borate.

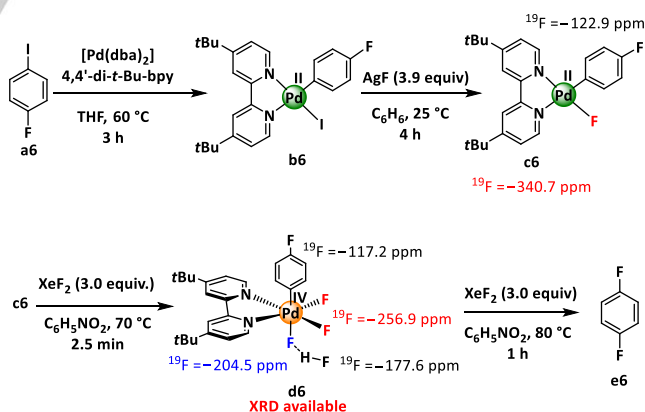
The authors hypothesized that, in the course of a $\text{S}_{\text{N}}2$ type mechanism, the formation of the cationic Pd(IV) complex **b4** occur by oxidative addition but unfortunately this latter could not be detected or isolated. According to the authors, this complex **b4** would rapidly undergo the reductive elimination reaction to form the cationic palladium (II) complex **c4** characterized in particular by a ^{19}F NMR signal at -300.0 ppm for the fluoride. The chemical shifts of palladium (II) monofluorides are typically in the range -270 ppm to -350 ppm.²⁶

The Ritter group synthesized the Pd(II) dinuclear dimeric complex **a5** both coordinated with benzo[*h*]quinoline and bridged by acetate ligands (Scheme 5).²³ The stoichiometric reaction of **a5** with a pyridylsulfonamide ligand led to the quick formation of a mixed mononuclear palladium (II) complex **b5**. The reaction of **b5** with 2.4 equiv of XeF_2 , similarly to Vigalok studies, allowed the oxidation of Pd(II) to Pd(IV) and the formation of the rather stable Pd(IV) difluoride complex **d5**. This complex could be analyzed and characterized by ^1H , ^{13}C and ^{19}F NMR. The ^{19}F NMR chemical shifts are very significant: the authors observed two signals at -169.2 ppm and -277.8 ppm, attributed respectively to an equatorial fluoride *trans* to a carbon atom ($\delta = -169.0$, $^2J_{\text{FF}} = 113$ Hz) and an axial fluoride *trans* to a nitrogen atom ($\delta = -278.0$). The complex **d5** is stable at room temperature for a week, and in chloroform solution at 50°C for 2 h. Complex **d5** crystallized from an acetonitrile solution as orange prisms and was analyzed by X-ray crystallography: the two fluoride substituents are in *cis* position and have bond lengths to palladium of $1.955(3)$ Å (axial) and $2.040(3)$ Å (equatorial). Heating of this difluoride **d5** at 150°C in dimethyl sulfoxide (DMSO) led to the reductive elimination of *N*-*ortho*-fluorinated benzo[*h*]quinoline **e5**. In order to get closer to the operational synthesis conditions for such electrophilic fluorination, the authors reacted **b5** with the more practical fluorinating agent Selectfluor.²³ An unstable cationic Pd(IV) intermediate **c5** was postulated from ^1H and ^{19}F NMR data. According to the authors, NMR resonances, including a ^{19}F NMR resonance at -278.0 ppm, are consistent with the axial fluoride **c5**; the instability of **c5** precluded isolation and purification for additional characterization. When the acetonitrile solution of **c5** was subsequently heated to 50°C , reductive elimination occurred to form **e5**. Additional evidence for the formation of a highvalent palladium fluoride was obtained when the intermediate **c5** was treated with tetramethyl ammonium fluoride tetrahydrate at room temperature to form the palladium (IV) difluoride **d5**.



Scheme 5. Pd(II) and Pd(IV) fluoride synthesis and *N*-ligand *ortho*-directed fluorination from reductive elimination.

The Sanford group extended their mechanistic studies to the formation of aryl fluorides (Scheme 6).²⁷ Palladium (II) precursor (*t*-Bu-bpy)Pd(*p*-FC₆H₄)(F) (**c6**) was prepared by sonication of (*t*-Bu-bpy)Pd(*p*-FC₆H₄)(I) (**b6**) with AgF . The fluorination of **c6** was monitored at lower temperatures by stirring with XeF_2 at 70°C for 2.5 min, which afforded the palladium (IV) complex **d6**. The ^{19}F solution NMR spectrum of **d6** at 25°C showed three broad resonances in a 1:1:2 ratios at -117.2 ppm (ArF), -206.3 ppm (axial F, *trans* to C), and -257.4 ppm (equatorial F, *trans* to N), respectively.



Scheme 6. Pd(II) and Pd(IV) fluoride synthesis and *N*-ligand *ortho*-directed fluorination from reductive elimination.

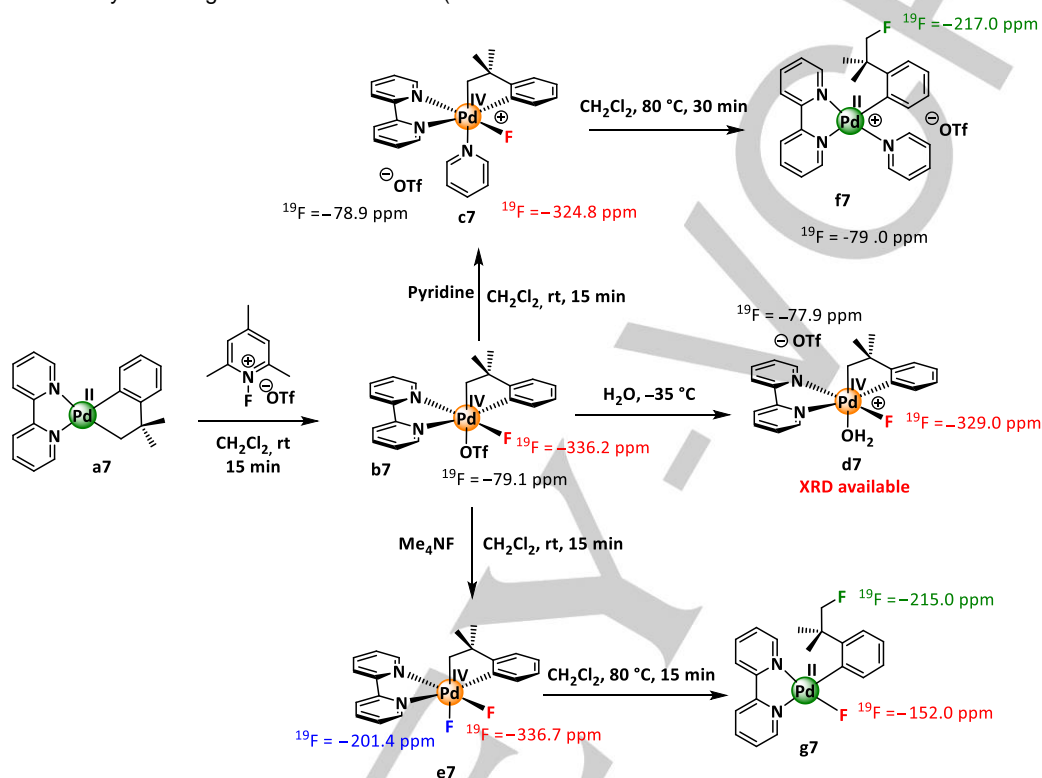
At -70°C , a fourth resonance was observed as a doublet of doublets at -177.6 ppm (HF) and the Pd–F peaks sharpened considerably and appeared as a multiplet (-204.5 ppm) and a doublet (-256.9 ppm). Structure of **d6** was confirmed by X-ray crystallography. The HF in this system was supposedly due to the reaction of XeF_2 with residual water. In contrast to Ritter group results, heating of this complex **d6** at 80°C for 1 h in nitrobenzene

MICROREVIEW

led to only traces of aryl fluoride **e6**. Instead, large quantities of biaryl homocoupling product were formed. The thermolysis of **d6** in the presence of XeF₂, *N*-fluorosulfanamide, and 1-fluoro-2,4,6-trimethylpyridinium tetrafluoroborate give the difluoroaryl product **e6** in major yield along with only traces of biaryl homocoupling product. Hypothetically, the complex mechanistic for this reductive elimination may involve FHF ligand. An additional important conclusion of this work is that direct C–F coupling from **d6** is slow relative to σ -aryl exchange between Pd centers (which

is the postulated pathway to Ar–Ar coupling). The aryl exchange process may be facilitated in this system because the σ -aryl group is *not stabilized* by a chelating moiety like in the *N*-directed processes of *ortho*-functionalization.

Following this work, Sanford group designed a system to access Pd(IV) alkyl fluoride complexes, and directly study their stoichiometric reactivity toward sp^3 -C–F bond formation by reductive elimination at Pd(IV) centers (Scheme 7).²⁸



Scheme 7. Synthesis and characterization of Pd(II)/Pd(IV) mono and difluoride complexes with a σ -alkyl ligand.

The oxidation of the cyclometalated bipyridine complex **a7** with *N*-fluoro-2,4,6-trimethylpyridinium triflate) afforded the Pd(IV) complex **b7** quantitatively. Complex **b7** react with pyridine or water to generate cationic complexes **c7** and **d7**, respectively. These three complexes are notably stable and could be stored in a freezer at -35 °C for several weeks. In the NMR of the complexes **b7-d7** the fluoride is coupled to one of the α hydrogen atoms of the σ -alkyl ligand ($J_{\text{FH}} = 15$ Hz) likely due to specifically oriented “through-space” spin-spin coupling.²⁹ This is confirmed by the X-ray structure solved for **d7** which additionally showed that the σ alkyl group of the cyclometalated ligand is in axial *trans* position to H₂O molecule. The difluoride **e7** was formed from triflate ligand displacement in **b7** and characterized with ¹⁹F NMR consistent with previously reported **d6** (Scheme 6). Both Pd(IV) complexes **c7** and **e7** underwent C–F bond-forming reductive elimination at 80 °C with high selectivity at sp^3 -C instead of sp^2 -aryl. DFT insights into the origin of the preference to form sp^3 -C–F over sp^2 -C–F bonds were conducted on this system and suggested that sp^3 -C–F coupling was kinetically favored of 7.0 to 13.0 kcal.mol⁻¹ for both complexes. Finally, C–F coupling could mechanistically occur either by direct reductive elimination or by dissociation of fluoride to generate a Pd(IV) (di)cation followed by

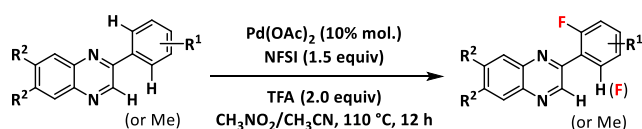
SN₂-type attack of F⁻ on the σ alkyl ligand; however, fluoride is generally a poor nucleophile for SN₂ reactions, and SN₂ reactions are typically slow in systems with high degrees of β substitution therefore direct C–F bond formation rather than SN₂-type attack on the Pd(IV) alkyl bond is likely. The above-described studies focused at identifying pertinent complexes and deciphering elementary steps of catalytic cycles through stoichiometric approaches. They paved the way towards catalytic development

2.3. Sub-stoichiometric approaches for palladium-catalyzed C–F bond formation

The Xu group developed a catalyzed fluorination reaction on derivatives of 2-phenylquinoxalines in the presence of Pd(OAc)₂, with *N*-fluorobenzenesulfonimide (NFSI) and trifluoroacetic acid (TFA) in a solvent mixture of nitromethane/acetonitrile (Scheme 8).³⁰ They extended these fluorination conditions on *para*-substituted pyrazole, benzo[d]oxazole and pyrazine derivatives. On this C–F bond formation conditions the authors have studied and proposed a mechanism for the *ortho*-directed fluorination of 2-phenylquinoxalines. First, they determined by kinetic measurements between 1 h and 12 h that difluorination occurred

MICROREVIEW

as soon as the monofluorinated arene was formed. Then, a clear primary kinetic isotope effect was observed in the intramolecular and intermolecular competition experiments with in both case $k_H/k_D \approx 2.3$, suggesting that the sp^2C-H activation is involved in the rate-limiting process. The authors performed mechanistic studies fluorination under sub-stoichiometric conditions using 0.5 equiv of $Pd(OAc)_2$ (50 mol%) with 1 equiv of 2-phenyl quinoxaline and 1.1 of NFSI, in the presence of 2 equiv of TFA. After one hour of reaction at 110 °C, the reaction medium was analyzed by mass spectrometry. The formation of a complex mixture of species was observed, with attribution of several palladium complexes as listed in Figure 2.³⁰



Scheme 8. 2-phenylquinoxalines mono and difluorination.

Cyclopalladation intermediates were detected at $m/z = 466$ ($[I + H]^+$), $m/z = 311$ (**I-1**), $m/z = 329$ (**I-2**), $m/z = 517$ ($[III + H]^+$), $m/z = 535$ ($[III-1 + H]^+$), and at $m/z = 553$ ($[II-2 + H]^+$). The presence of $-N(SO_2Ph)_2$ ligands (presumably formed after fluorination reaction or alternatively by destruction of NFSI) coordinated to Pd(II) atom was also observed within several complexes attached to various ancillary components: at $m/z = 608$ ($[IV-1 + H]^+$) and $m/z = 626$ ($[IV-2 + H]^+$), at $m/z = 649$ ($[IV-3 + H]^+$) and $m/z = 667$ ($[IV-4 + H]^+$) with CH_3CN solvent, at $m/z = 814$ ($[IV-5 + H]^+$) with quinoxaline substrate, and at $m/z = 832$ ($[IV-6 + H]^+$) and $m/z = 850$ ($[IV-7 + H]^+$) with fluorinated phenylquinoxaline.

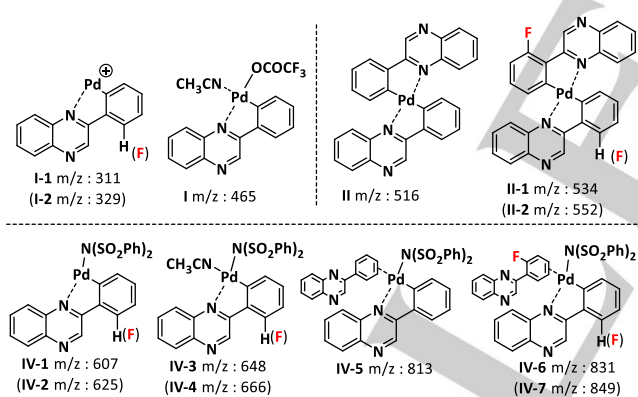
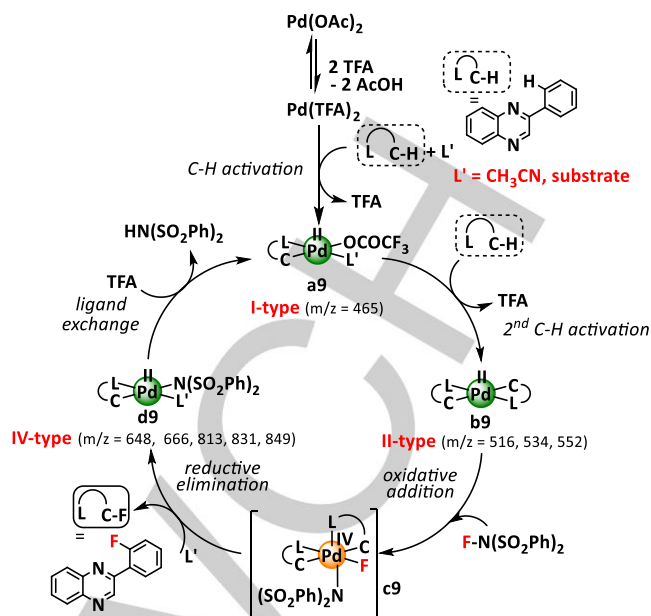


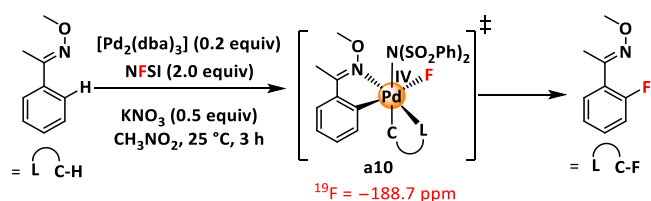
Figure 2. Mass-analysis of sub-stoichiometric mixture (adapted from ref. 30) with Pd(II) species identified by tandem mass spectrometry (MS/MS) experiments.

Based on these experiments, and on the above-discussed stoichiometric mechanistic studies on C–F reductive elimination from high-valent palladium(IV) fluoride, the authors proposed a plausible catalytic cycle involving Pd(II)/Pd(IV) species (Scheme 9).³⁰



Scheme 9. Catalytic cycle for 2-phenylquinoxalines fluorination.

From $Pd(OAc)_2$ a ligand exchange between acetate and TFA occurs initially to lead to the formation of $Pd(TFA)_2$. Then, a molecule of quinoxaline coordinates with palladium and undergoes a C–H activation to form **a9** (I-type, in Figure 2). Complexes like **a9** had been identified by MS/MS in the related sub-stoichiometric studies (Figure 2). The palladium complex **b9** is formed after coordination of a 2nd molecule of quinoxaline to **a9** by C–H activation with TFA (Scheme 9). **b9** is a complex of II-type also detected by MS/MS. It was assumed then that addition of NFSI on this complex **b9** leads to the oxidation of palladium to form Pd(IV) intermediate **c9**. This oxidizing addition is directly followed by a fast reductive elimination allowing the release of the desired fluorinated product and a Pd(II) complex **d9** of IV-type (detected in MS/MS, Figure 2) coordinated to a molecule of quinoxaline and residual $N(SO_2Ph)_2$. A molecule of TFA may replace the ligand $N(SO_2Ph)_2$. This leads to the formation of $HN(SO_2Ph)_2$ and regeneration Pd(II) complex **a9**. The addition of this TFA molecule also temporarily disfavors the difluorination of quinoxaline derivatives improving the global selectivity of the process. The overall cycle is consistent but no direct evidence of the formation/involvement of the Pd(IV) complex **c9** was provided. Therefore, the hypothesis of an outer Pd(II) sphere attack of NFSI could not be fully ruled out at this stage (see also section 4). Xu and co-workers then reported a related fluorination reaction of O-methylated aryl oxime ethers in the presence of $[Pd_2(dba)_3]$ (or $Pd(OAc)_2$), NFSI and KNO_3 (or $AgNO_3$) in nitromethane at 25 °C (Scheme 10).³¹



Scheme 10. Pd(IV)–F fluoride complex **a10**.

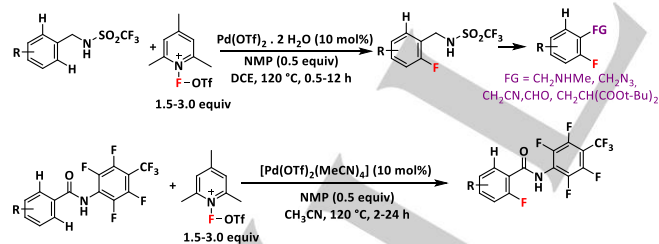
The authors proposed a Pd(II)/Pd(IV) mechanism similar as the one depicted in Scheme 9 (oxime substrate replacing

MICROREVIEW

quinoxaline), except that the NO_3 ligand replaced TFA, and that is initiated by a cationic $[\text{Pd}(\text{NO}_3)]^+$ species. The authors conducted a sub-stoichiometric mechanistic approach on the fluorination of aryl oxime ethers. One equiv of (*E*)-acetophenone *O*-methyl oxime was reacted with 0.2 equiv of $[\text{Pd}_2(\text{dba})_3]$, 2.0 equiv of NFSI and 0.5 equiv of KNO_3 in nitromethane. After 3 h of reaction, NMR and mass spectrometry analyzes were performed on the mixture which allowed the unambiguous identification of Pd(II) complexes resulting from the expected cyclopalladation with oxime. Mass analysis was less accurate concerning the supposed Pd(IV) (no tandem MS/MS analysis) and a signal detected at $m/z = 718$ that may correspond to the Pd(IV)-F complex **a10** (Scheme 10) is unfortunately lacking the isotopic distribution of palladium (Pd^{104} 11 %, Pd^{105} 22 %, Pd^{106} 27 %, Pd^{108} 26 %, Pd^{110} 11 %) to be fully convincing. Nevertheless, in ^{19}F NMR a chemical shift $\delta = -188.7$ ppm was clearly observed, which might correspond to a fluorine atom bound to Pd(IV). This, consistently with the Pd(IV) difluoride complex **d5** (Scheme 5) isolated by Ritter group, in which a ^{19}F NMR chemical shifts observed at -169.2 ppm was attributed to an equatorial fluoride *trans* to a carbon atom further identified by XRD.³² In this work the functionalization conducted at room temperature is a significant experimental advance for C–H fluorination. While the nitrate anion was found to be the crucial promoter of room temperature fluorination, its actual function is still not clear, and should be further studied in upcoming mechanistic studies.

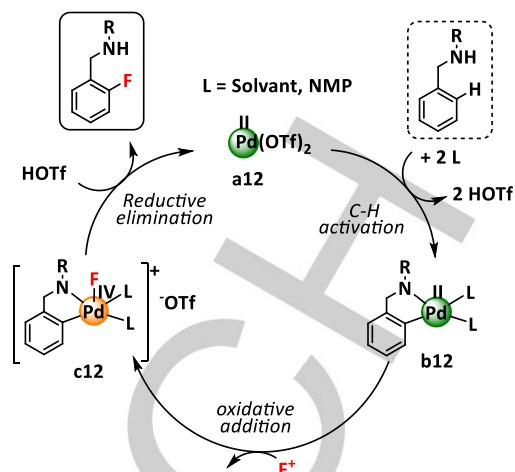
2.4. Experimental advances with related catalytic cycle proposals

The Yu group reported on the sp^2 -C fluorination of *N*-benzylamine derivatives and *N*-arylbenzamides (Scheme 11).³³ The use of *N*-fluoro-2,4,6-trimethylpyridinium triflate as the F^+ source and NMP (N-methyl-2-pyrrolidone) as a promoter is crucial for this reaction. A significant advance was the further straightforward conversion of directing groups into synthetically useful functional groups, giving access to *ortho*-fluorinated compounds including benzaldehyde, benzylamine, benzylazide, phenylacetone, and phenylpropanoate groups.



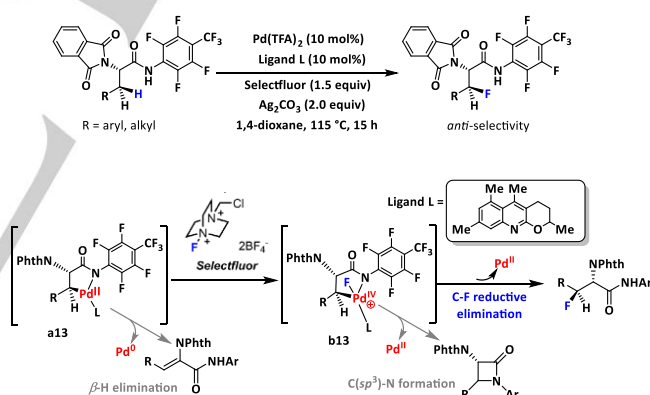
Scheme 11. sp^2 -C Fluorination of *N*-benzylamine derivatives and *N*-arylbenzamides.

In the absence of further supporting data, the authors proposed a catalytic cycle (Scheme 12), in which the detailed role of NMP remains to be elucidated. They based their cycle on the investigations by Vigalok and Ritter groups (Schemes 4 and 5, respectively) which proposed that oxidation of L_2PdArI by a F^+ source *via* an $\text{S}_{\text{N}}2$ -type mechanism gives a low-stability cationic pentacoordinated $\text{L}_2\text{Pd(IV)ArIF}$ intermediate that undergoes fast reductive elimination (c12 in Scheme 12).



Scheme 12. Catalytic cycle for *ortho*-benzylamine fluorination.

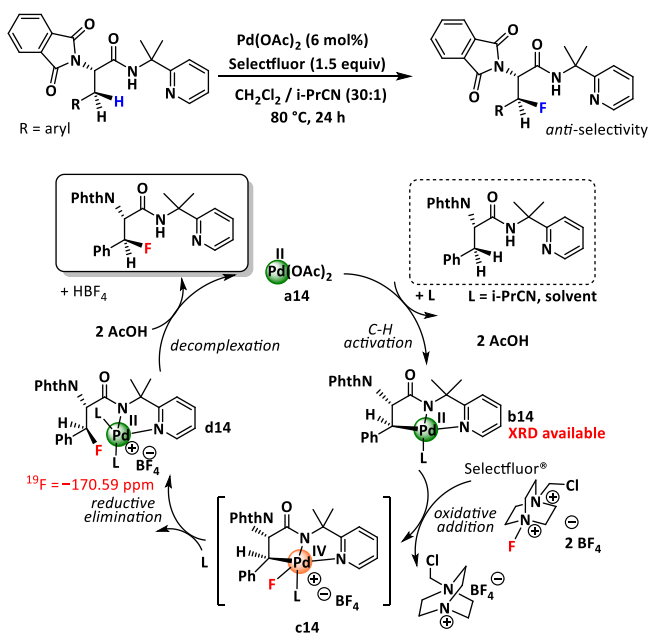
The Yu group extended their studies to *L* ligand-assisted stereoselective β -C(sp^3)-H fluorination, enabling the synthesis of enantiopure *anti*- β -fluoro- α -amino acids with *anti/syn* d. r. generally $>20:1$ (Scheme 13).³⁴ In the classical catalytic cycle proposed by the authors (analogous to Scheme 12), while the exact role of the ligand *L* remains to be studied, the ligand effect is essential in favoring the C(sp^3)-F bond forming reductive elimination over the intramolecular C(sp^3)-N bond-forming reductive elimination in the postulated intermediate **b13** (Scheme 13). Another side reaction which was not detected is the β -H elimination from the postulated intermediate **a13**.



Scheme 13. Stereoselective β -C–H fluorination of α -amino acid *L*-phenylalanine amide derivatives intermolecularly assisted by *L* ligand.

Shi and coworkers developed in parallel a mild procedure for synthesizing *anti*- β -fluoro- α -amino acids with full diastereoselectivity (the authors mentioned that *syn* stereoisomer could not be detected) in the conditions shown in Scheme 14, in which addition of ligands is unnecessary.³⁵ This because the directing group is *N,N'*-bidentate and probably provides an additional stability to the catalytic system.

MICROREVIEW

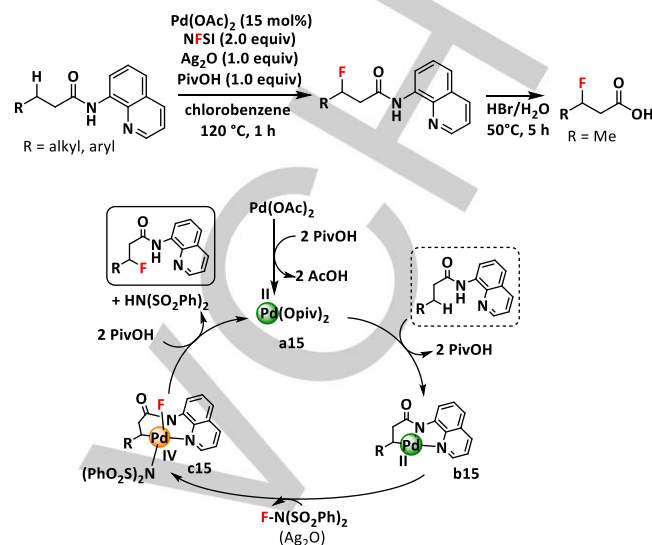


Scheme 14. Stereoselective β -C–H fluorination of α -amino acid L-phenylalanine amide derivatives intramolecularly induced.

The procedure initially focused at benzylic species (R = aryl) was extended to aliphatic substrates by using 10 mol% Pd(OPiv)₂ and 0.2 equiv of the acid additive 2-methylbenzoic anhydride (2-Me-BAH).³⁵ The exact role of this additive remained unclear. In the case of the C–H fluorination of benzylic methylene in these amino acid derivatives, the authors proposed a catalytic mechanism based on a step-by-step stoichiometric study (Scheme 14). A palladacycle(II) type **b14** was synthesized and fully characterized (NMR, XRD) showing the correct conformation for further *anti*-fluorination. Upon addition of 1.05 equiv of Selectfluor in *d3*-MeCN, **d14** was quickly formed in 5 to 10 min, and was characterized in ^1H NMR (δ β -H = 6.52 ppm, $^2J_{\text{HF}} = 46.8$ Hz and (δ α -H = 5.50 ppm, $^3J_{\text{HF}} = 15.6$ Hz) and ^{19}F NMR by a shift $\delta = -170.59$ ppm (vs $\delta = -167.10$ ppm in the final uncoordinated product). They finally showed that isolated **b14** (6 mol%) was catalytically competent for C–H fluorination provided AcOH (12 mol%) was added.

The non-stereoselective fluorination of C(*sp*³)-H bond on β -alkyl amides directed by a 8-aminoquinoline group was also achieved by Xu and coworkers using the fluorinating agent NFSI, assisted by pivalic acid (PivOH) and Ag₂O (Scheme 15).³⁶ They

hypothesized a cycle inspired by the previously discussed mechanistic studies. In the absence of further investigation, they proposed that Pd(II) is oxidized into a Pd(IV) intermediate by NFSI and Ag₂O that is necessary for this reaction to proceed.



Scheme 15. Synthetic pathway to β -fluorinated carboxylic acids.

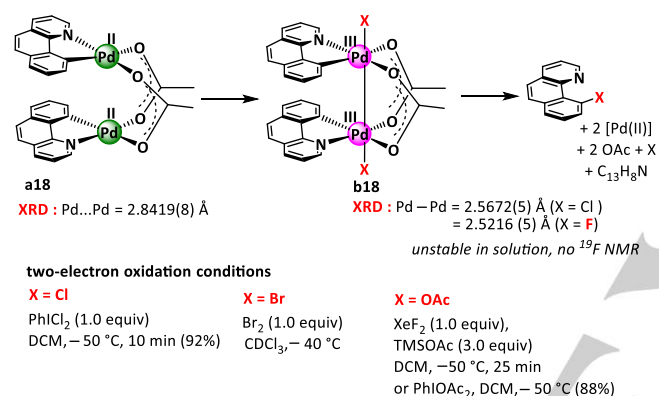
The Liu group developed a palladium-catalyzed oxidative aminofluorination of vinyl arenes, in which NFSI functionalized the double bond both as a fluorination and an amination reagent (Scheme 16, top).³⁷ The reaction afforded vicinal fluoroamine products with very high regioselectivity. A detailed mechanistic proposal was provided (Scheme 16, bottom). Stoichiometric investigation monitored by ^{19}F NMR, ^1H NMR and ESI-MS spectroscopy suggested that Pd(0) complex **a16** formed with bathocuproine (BC) is oxidized by NFSI to afford the palladium(II) complex **b16** (characterized by $\delta^{19}\text{F}$ NMR at -381 ppm³⁸). Complex **b16** can quickly react with styrene to afford the styrene aminofluorination product. From the stoichiometric reaction between (BC)Pd(OAc)₂ and NFSI, there are no new signal observed in the ^{19}F NMR spectrum and no aminofluorination of styrene occurred at room temperature when styrene was added. The reaction only occurred at 50 °C. Those results suggested that the aminofluorination of styrenes is specifically initiated by (BC)Pd(0) species, which possibly derived from the reduction of (BC)Pd(OAc)₂ by styrene.

MICROREVIEW

3. Bimetallic Pd(III)/Pd(III) species in C–X bond formation

3.1. Experimental stoichiometric approaches: kinetics and structures

The Ritter group reported carbon–chlorine C–Cl, carbon–bromine C–Br and carbon–oxygen C–O reductive elimination from discrete bimetallic Pd(III) complexes (Scheme 18). These were the first recognized organometallic reactions from Pd(III), which led to propose bimetallic Pd(III) catalysis as a mechanistic alternative to monometallic Pd(II)/Pd(IV) redox cycles.⁴⁰ Later, Pd(III) difluoride complex **b18** has been isolated in the solid state alongside crystals of extended Pd(III) chain structures.^{40b} However, crystals of **b18** dissolved as Pd(III) chains and did not lead to fluorinated products. Thus, Pd(III) catalysis has not been discussed in depth for electrophilic fluorination. However, linking Pd(III) to other palladium oxidation states is reasonable, and as such deserves a brief review here.

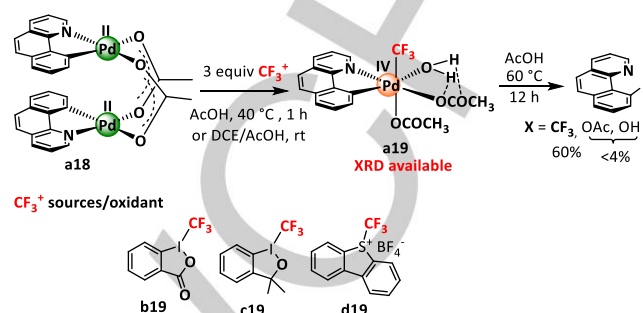


Scheme 18. Bimetallic Pd(III)–Pd(III) palladacycles formation and reactivity in C–X formation (X = Br, Cl, O).

Cyclopalladation from benzo[h]quinoline gives the bimetallic Pd(II) complex [(bzq)Pd(OAc)₂]₂ **a18** (Scheme 18). Two-electron oxidation of complex **a18** with oxidants (such as PhICl₂ or PhI(OAc)₂) oxidizes each palladium atom by one electron, which results in the complex **b18** with a Pd(III)–Pd(III) single bond. During bimetallic reductive elimination from **b18**, an overall two-electron process occurs in which each palladium atom is reduced by one electron with concomitant cleavage of the Pd–Pd bond. Sanford group reported a detailed kinetic analysis of a Pd(OAc)₂-catalyzed oxidation (arylation C–C coupling) with I(III) diaryliodonium salts.⁴¹ They reported a second-order dependence for a rate-limiting step which would be the oxidation of a Pd(II) dimer (type **a5**) to higher oxidation binuclear palladium intermediates formulated either as [Pd(II),Pd(IV)] or [Pd(III)–Pd(III)].

However, shortly after the Sanford group described the oxidation of cyclometalated Pd(II) dimer [(bzq)Pd(OAc)₂]₂, **a18** (Scheme 19), with electrophilic trifluoromethylation (CF₃⁺) reagents to generate monomeric Pd^{IV} trifluoromethyl aquo complex **a19**.⁴² This complex was found to be a kinetically competent catalyst for *sp*²-C–CF₃ bond formation. The formation of this complex, which was isolated and characterized by XRD in the solid state, established that Pd(II) dimers can also evolve towards monomeric Pd^{IV} species. Interestingly, in the solid state the aquo ligand is *trans* to the σ -aryl group, and presents two intramolecular hydrogen bonds with the oxygen atoms of the

acetate ligand in position *cis*. These H-bonding interactions were proposed to be at the origin of the chemoselectivity of **a19** for C–CF₃ bond formation versus minor concurrent C–O bond reductive elimination (<4%). The other important point is that in this reaction, acidic additives (Brønsted or Lewis acids: trifluoroacetic acid TFA⁴³ or anhydride TFAA, and Yb(OTf)₃) increased the rate, yield and mass balance of C–CF₃ bond forming reductive elimination.



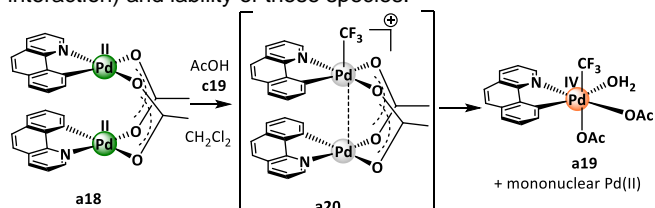
Scheme 19. Dinuclear Pd(II) to mononuclear Pd(IV) evolution from oxidation with electrophilic trifluoromethylating reagents.

These results raised interrogations regarding the generality of binuclear or mononuclear palladium intermediates in such catalytic oxidation reactions. And this especially in the case of electrophilic fluorination we review herein since this specific reaction has not been achieved (see the use of XeF₂ in Scheme 18) under the oxidation conditions developed by the groups of Ritter, Sanford and others.

Following these results, deeper understanding of the roles of mononuclear Pd(IV) and binuclear Pd(III) intermediates in oxidation during palladium-catalyzed *N*-directed electrophilic functionalization was further pursued cooperatively by Ritter, Sanford, Canty and Yates groups.⁴⁴ Since under similar stoichiometric oxidation conditions binuclear Pd(III) (Scheme 18) or mononuclear Pd(IV) (Scheme 19) high oxidation palladium intermediates have been formed, the *potential interconversion between these structures* was examined.⁴⁴ No reaction intermediates were observed by NMR (¹H and ¹⁹F) during the oxidation of **a18** to **a19** and the authors then measured initial rate kinetics to gain insight into the relative timing of oxidation and/or mononuclear fragmentation reactions. The initial rate of oxidation was found to be $r = k[\mathbf{a18}][\mathbf{c19}][\text{AcOH}]$.^{44, 45} The rate was determined to be first-order dependent on the concentration of binuclear Pd(II), oxidant **c19** and acetic acid. According to the authors, if dissociation of **a18** to afford two equivalent mononuclear species were to precede a rate-determining oxidation a reaction order of ½ with respect to **a18** would be expected. Another important point was the dependence of the reaction rate on [AcOH] but not on [AcO[–]], which is consistent with protonation of **c19** to generate a more potent oxidant (indirect evidences of this protonation is given from ¹⁹F NMR downfield shift monitoring), and justify the impact of acidic additive previously observed by Sanford group. Overall, the rate law for oxidation of **a18** is consistent with an oxidized binuclear Pd complex **a20** as the immediate product of oxidation of **a18** (Scheme 20). According to the authors, the nature of Pd(III)–Pd(III) or Pd(II)–Pd(IV) of **a20** is formally difficult to assess in relation with the “*subtleties of formal oxidation state assignment for unsymmetrical binuclear Pd(III) species*”. The related Canty and Yates theoretical investigation (further details in next section) early on suggested that the apical ligands in such Pd...Pd

MICROREVIEW

bimetallic systems influence the geometry (metal/metal interaction) and lability of these species.⁴⁶



Scheme 20. Mononuclear Pd(IV) formation from dinuclear Pd(II) via binuclear cationic **a20** undergoing disproportionation (bimetallic oxidation / Pd–Pd cleavage).

Finally, as it was mentioned by the authors,⁴⁴ palladium-catalyzed electrophilic trifluoromethylation quantitative kinetics were complicated by the presence of an induction period (suppressed by Brønsted and Lewis acids) for RE from **a19**, which suggests that the mechanism of C–CF₃ bond formation is more complicated than direct RE from **a19**.⁴² Accordingly, while binuclear formally Pd(III) and mononuclear Pd(IV) chemistry can be related by Pd–Pd bond cleavage, this feature does not fully elucidate the palladium complex structure from which C–CF₃ bond formation proceeds. Nevertheless, the above discussed results collectively remain among the most advanced experimental studies to be considered in the forthcoming mechanistic investigations of palladium-catalyzed electrophilic fluorination reactions and its nuclearity.

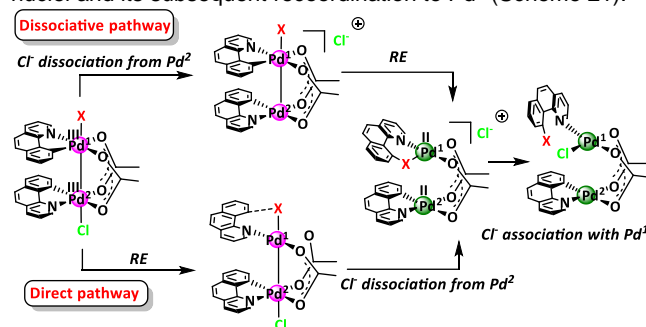
3.2. Theoretical approaches focused at bimetallic palladium complexes and intermediates reactivity

Until 1998 and the work of Cotton group,⁴⁷ the number of compounds of Pd(III) that have been isolated and characterized was scarce. For instance, in seminal works [Pd₂(DTolF)₄], where DTolF- is [(*p*-tolyl)NC(H)N(*p*-tolyl)]⁻, had been tentatively oxidized to [Pd₂(DTolF)₄](PF₆), which was crystallographically characterized, with a Pd...Pd distance of 2.637(6) Å, only slightly longer from that, 2.622(3) Å, in the starting material (ligand rather than M₂ core oxidation occurs).⁴⁸ Conversely, the nitrogen-donor ligand hpp (anion of 1,3,4,6,7,8-hexahydro-2H-pyrimido[1,2-*a*]pyrimidine) was reacted with Pd(OAc)₂ in THF to produce the dimeric Pd(II) orange complex [Pd₂(hpp)₄], which upon two-electron oxidation with PhCl₂ resulted in the formation of the dark complex [Pd₂(hpp)₄Cl₂].⁴⁷ The structures of these complexes are very similar with two palladium atoms which are bridged by four hpp ligands, resulting in a paddlewheel-type structure. Additionally, two axial chloride ions are present in [Pd₂(hpp)₄Cl₂]. While there is formally no metal-metal bond in [Pd₂(hpp)₄] (although the intermetallic separation is quite short, Pd...Pd = 2.555(1) Å) the short Pd–Pd bond distance of 2.391(2) Å found in [Pd₂(hpp)₄Cl₂] was attributed to the first X-Ray characterized Pd(III)–Pd(III) complex.^{45b} To investigate the Pd–Pd bond formed, the authors performed calculation of the electronic structure of the [Pd₂(hpp)₄Cl₂] molecule (Hartree-Fock method), in which the geometry was optimized, giving results in excellent agreement with experiment: Pd–Pd, 2.402 Å vs 2.391 Å (observed) and for the torsion angle 22.6° vs 24°(observed).⁴⁷ The HOMO and LUMO contours analyzed in the plane formed by the Cl–Pd–Pd–Cl unit and four nitrogen atoms from two hpp ligands evidenced that the Pd–Pd bond is a σ -bond formed mainly by a $d_{z^2} - d_{z^2}$ overlap.

Following these results, the Ritter group reported bimetallic symmetrical complexes of formula **b18** (see previous section) in which [X–Pd(III)–Pd(III)–X] motif with metal-metal bond was ascertained.⁴⁹ From single crystal structure when X = OAc, Pd–Pd = 2.5548(5) Å (vs 2.5672(5) Å when X = Cl, see Scheme 18). Joint experimental and computational studies from Ritter and Goddard group attempted to elucidate whether the core of dinuclear Pd(III) complex stay intact during reductive elimination in low polarity solvent CH₂Cl₂.⁵⁰ The presence of the second metal in dinuclear complex **b18** (X = Cl) lowers the activation barrier of reductive elimination. When reductive elimination is forced to proceed via a monometallic pathway by eliminating metal-metal communication, the barrier to reductive elimination is increased by ca 30 kcal.mol⁻¹.

Canty, Yates and coworkers then predicted from density functional theory investigation (DFT) important ligand effects in bimetallic high oxidation state systems based on unsymmetrical [X–Pd–Pd–Y] motif.⁴⁶ Such systems are very likely to operate in Pd-catalyzed oxidation reactions, including electrophilic fluorination. The ligand X has a strong effect on the dissociation reaction of ligand Y to form the cationic species [X–Pd–Pd]⁺ + Y⁻. If Y is a weak σ -donor ligand and a good leaving group (Cl, Br, I, CN, F), dissociation of Y is facilitated by greater σ -donor character of X (SiMe₃, C(O)Me, Me, Ph, etc.) relative to Y. A linear correlation of the Pd–Y and Pd–Pd bond lengths was observed with Pd–Y bond dissociation energy, and with the σ -donating ability of X. These results were explained by the fact that the Pd d_{z^2} population in the [PdY] fragment increases as the donor ability of X increases. In such binuclear systems, thus the Pd(III)–Pd(III) arrangement is favored when X is a weak σ -donor ligand (such as F, Cl or OAc), while a more accurate Pd(IV)–Pd(II) arrangement is predicted when X is a strong σ -donor ligand (such as SiMe₃, Me or Ph). Interestingly, high polarity solvent was predicted to favor such ligand exchanges that contribute to the formation of bimetallic cationic species in which each palladium atom is six-coordinate; highly polar media being clearly preferred in the related catalytic reactions.

The question of the influence of solvent polarity was reinforced by a follow-up theoretical study by Canty and Yates group which indicated the presence of a competing dissociative pathway in polar media. DFT calculations were performed to investigate the mechanism of formation of C–Cl and C–C bonds via reductive elimination (RE) from classical dimeric organopalladium complexes [(L-C,M)XPd¹-(μ -OAc)₂Pd²Cl(L-C,M)] either through a dissociative (cationic RE) or a direct pathway (neutral RE). According to these calculations, the direct pathway reductive elimination first occurs followed by the Cl dissociation from Pd² nuclei and its subsequent recoordination to Pd¹ (Scheme 21).



Scheme 21. Dissociative pathways preferred for C–C bond formation (X = Ph, in CH₃CN or CH₂Cl₂) and C–Cl (in CH₃CN); direct pathway preferred for C–Cl bond formation in CH₂Cl₂.

MICROREVIEW

In the dissociative pathway, loss of Cl^- yields a cationic bimetallic species, which undergoes reductive elimination, and then subsequent Cl^- recoordination to Pd1. In the dissociative pathway, the reductive elimination occurs with electron-transfer into the d_z^2 orbitals on Pd¹ and Pd². This process leads to the breaking of the Pd–Pd bond, and concomitant change of oxidation state from Pd(III)–Pd(III) to Pd(II)...Pd(II). Overall, for bimetallic complexes where X = Ph the dissociative pathway is more favorable regardless of the solvent polarity because of the weakness of Pd²–Cl bond. Concerning bimetallic complexes where X = Cl the direct pathway is more favorable when a low polarity solvent is used, while in high polarity solvents the dissociative pathway becomes competitive in relation with the adequate solvation of the charged species. According to Canty and Yates, finally the reductive elimination step from the neutral bimetallic complexes is more difficult than from the cationic bimetallic complex because the process of populating the LUMO+1 in the direct reductive elimination from neutral bimetallic complexes requires greater deformation energy.

Schoenebeck *et al.* reported from spectroscopic and computational studies of the stoichiometric reactivity from a mixed Cl/OAc dinuclear Pd(III) complex that the mixed dinuclear Pd(III) complex scrambles readily to give the two Pd(III) homodimers of which the dichlorinated Pd(III) dimer ultimately gives *ortho*-chlorinated aryl upon reductive elimination.⁵¹ All these important general questions relating to bimetallic/monometallic species remain mostly opened for the specific conditions concerning electrophilic fluorination reactions.

Most recently, Musaev studied the general factors controlling stability and reactivity of dimeric Pd(II) complexes in C–H functionalization catalysis.⁵² Experimental and computation indicates that the most stable form of Pd-acetate in the absence of coordinating ligands is the trimeric complex $[\text{Pd}(\text{OAc})_2]_3$. The trimer/dimer equilibrium $2/3 [\text{Pd}(\text{OAc})_2]_3 \rightleftharpoons [\text{Pd}(\text{OAc})_2]_2$ is unfavorable by 15.1 kcal.mol⁻¹, a value which is small enough to be overcome by ligation and solvation effects. Thus, $[\text{Pd}(\text{OAc})_2]_2$ may have several different isomeric forms but clearly, bridging acetate ligands (studied over zero, two, or four bridging ligands) increases the stability of the dimer. Modeling idealized Pd(II)...Pd(II) interaction shows that there should not be formal bonding between the Pd(II) atoms. However, mixing of the filled Pd(II)–Pd(II) $d\sigma^*$ antibonding orbital with the unoccupied Pd s and p_z orbitals creates a hybridized orbital with less antibonding character and introduces some degree of interaction between the metal centers. The degree of Pd $d\sigma^*/s/p$ mixing, and therefore the degree of Pd–Pd bonding depends critically on the Pd...Pd distance as well as the electronic nature of the bridging ligands. Accordingly, calculated Wiberg bond index (WBI) values are small but nonzero and increase in the same order as the Pd–Pd distance. Palladium acetate dimer is more stable than separated monomers due to the interactions between the paddlewheel ligands and the palladium center and a Pd–Pd interaction contributes to the stability of the dimeric $[\text{Pd}(\text{OAc})_2]_2$ structure to a minor extent.⁵²

The factors affecting the electron-rich and -poor nature of the bridging O-centers determine the stability of the $[\text{Pd}(\text{O}_2\text{CR})_2]_2$ dimers. Thus, R-substitution in $[\text{Pd}(\text{O}_2\text{CR})_2]_2$ which leads to an increase in the σ -electron-density of the ligand orbitals, polarizes the Pd–ligand interaction and weakens the stability of the $[\text{Pd}(\text{O}_2\text{CR})_2]_2$ dimers relative to the monomers by a destabilizing

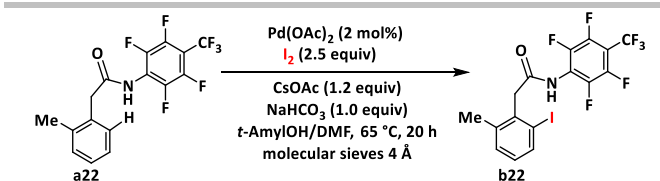
effect linked to reduced Pd–Pd distances. On the other hand, a decrease in the σ -electron density on the ligand would increase the positive charge on the Pd centers, increase electrostatic repulsion between them, and consequently, elongate the Pd–Pd distance towards dimer stabilization. The trends are complicated for the R-group with π -donating or -withdrawing effects.⁵² Finally, Musaev group reported that starting from the dinuclear $[\text{Pd}(\text{OAc})_2]_2$ complex, the monomer formation from $[\text{Pd}(\text{OAc})_2]_2$ and C–H activation by the dimer complex compete with each other: in general, the dinuclear complexes require a higher C–H activation barrier than the mononuclear complexes. However, the C–H functionalization process may proceed via a dimeric $[\text{Pd}(\text{OAc})(\text{DG-Ar})]_2$ complex, especially for systems with strongly interacting substrates (via for instance π – π stacking) and smaller palladacycles (5-membered palladacycles formed more stable dimeric complexes than 6-membered palladacycles), and electrophiles having small C–X bond formation barriers. This probably distinguishes the case of C–H iodination (by Yu group, see details in section 4) and C–H chlorination (by Ritter group, above discussed).

This set of studies altogether tends to demonstrate that a unified mechanistic picture for *ortho*-C–H bond electrophilic functionalization encompassing C–C, C–O and C–*hal* (*hal* = I, Br, Cl, F) bond formation from Pd-acetate oxidation chemistry is far from being reached. However, a number of critical factors and their respective effects have been identified and studied such as mainly: (pre)-catalyst nuclearity, solvent polarity, ionic or neutral nature of the intermediates, effects of the oxidation and electrophilic reagents, role of additional acidic additives, dimeric species stability in relation with Pd...Pd interaction. These studies also evidenced the difficulties of identifying genuine structures of d catalysts, and some unexpected limitations within the formalism of Pd dimers oxidation state. However, they also resulted in the isolation and unambiguous characterization of original and pertinent complexes, which may stimulate additional research to address the potential of palladium C–H electrophilic functionalization catalysis.

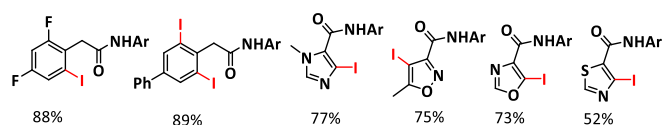
4. “Outer sphere” processes

In this section we gathered under the name “outer sphere” processes several alternative mechanisms in which the C–H functionalization step only partially depends on the Pd center – whatever its formal oxidation state is– because of outer interactions and processes. In this context, $[\text{Pd}(\text{I})/\text{Pd}(\text{II})]$ redox-neutral mechanisms are worth mentioning. In 2013, Yu group reported a Pd-catalyzed *ortho*-C–H iodination directed by a weakly coordinating amide auxiliary using I_2 as the sole oxidant.⁵³ This large-scope reaction achieved with functionalized arenes was found to be also compatible with a wide range of heterocycles including pyridines, imidazoles, oxazoles, thiazoles and pyrazoles (Scheme 22).

MICROREVIEW

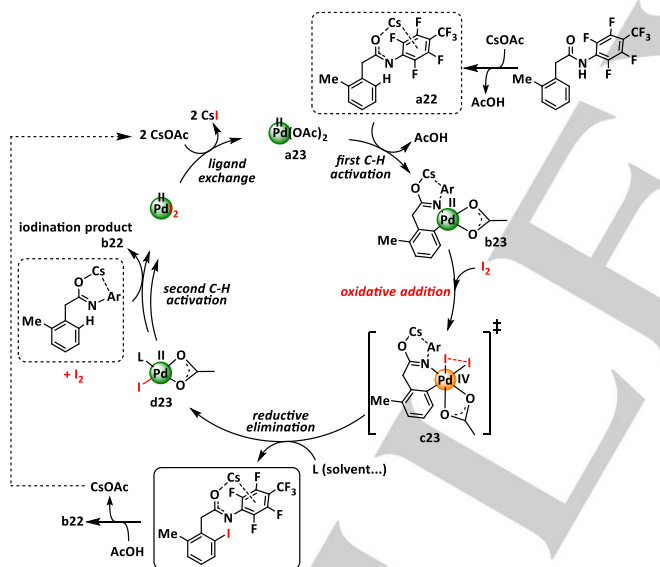


Selected examples:



Scheme 22. Pd-catalyzed *ortho*-C–H iodination directed by a weakly coordinating amide.

The authors studied the mechanism and governing factors of Pd(II)-catalyzed C–H iodination with I_2 as oxidant (Scheme 22), focusing at comparing a Pd(II)/Pd(IV) redox pathway [called oxidative addition (OA)] (Scheme 23) and a Pd(II)/Pd(II) redox-neutral pathway [called electrophilic cleavage (EC)] (Scheme 24) for the iodination step of this reaction.⁵⁴ The authors carefully computed all the reaction steps, in relation with experimental observation and taking into accounts a number of parameters like the influence of potential dimers (for simplicity monomers are depicted), the role of the exogenous base additives, *etc.* These details are not discussed herein but are of great interest to examine for a more in depth approach.⁵⁴

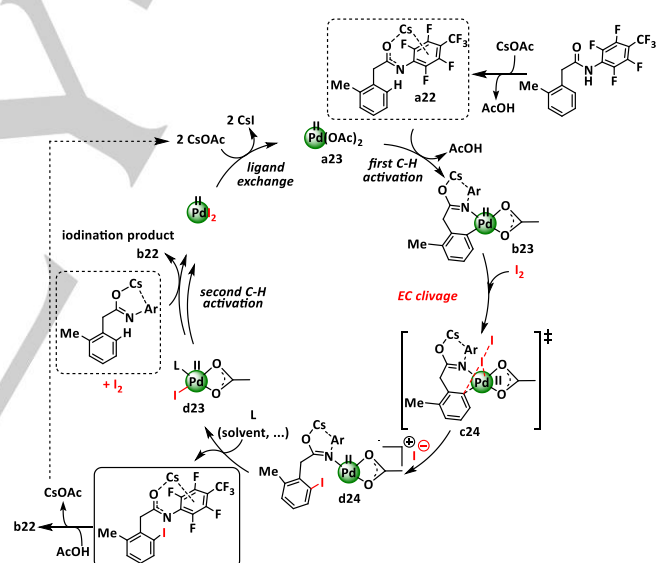


Scheme 23. Catalyzed C–H iodination with I_2 as oxidant following a Pd(II)/Pd(IV) redox pathway.

First, the reaction was conducted in the presence of CsOAc salt. The deprotonation of the HN-amide group of RCONHAr substrates by the Cs was necessary for its optimal coordination to the Pd(II)-center. NMR and computational data have suggested that the strong electron-withdrawing substituents on the N-Ar group such as $(4-CF_3)_2C_6F_4$, increase the acidity of the amide N–H bond and make the reactive deprotonated amide species widely available. After deprotonation the Cs^+ counter ion would stay weakly coordinated to the π -electronic density of the $[OCNAr]^-$ fragment. Next, coordination of the deprotonated substrate to monomeric $Pd(OAc)_2$ would lead to the formation of the complex $[PhCH_2-CONArCs]-Pd(OAc)_2$. The next step of the reaction,

which is redox-neutral, would be aryl C–H bond activation that proceeds via the concerted metalation–deprotonation mechanism (CMD) to yield palladacycle **b23** (Schemes 23 and 24). This step requires a barrier of $14.3 \text{ kcal}\cdot\text{mol}^{-1}$ and is exergonic by $10.9 \text{ kcal}\cdot\text{mol}^{-1}$ (calculated relative to $[PhCH_2-CONArCs]-Pd(OAc)_2$). Calculations showed that the dimerization of the palladacycle **b23** is favorable by $5.0 \text{ kcal}\cdot\text{mol}^{-1}$ indicating that dimers can play a significant role in the reactions following the C–H activation.⁵⁴

After the C–H activation, I_2 coordinates to the d^8 -Pd(II) palladacycle, **b23** (or its dimer analogs). Extensive calculations of I_2 coordination to **b23** resulted in two structurally and electronically different I_2 adducts, **c23** (Scheme 23) from OA and **c24** (Scheme 24) from EC. Importantly, the origin of this two different approaches were related to the fact that I_2 molecule, with the frontier electronic configuration of $[(1\sigma_g)^2(1\sigma_u^*)^2(2\sigma_g)^2(2\pi_u)^4(2\pi_g^*)^4(2\sigma_u^*)^0]$ may act either as an electron *acceptor* to the empty $2\sigma_u^*$ orbital (LUMO) or an electron *donor* from the filled $2\pi_g^*$ orbital (HOMO). As an electron-accepting ligand, I_2 interacts with the doubly occupied d_{z^2} orbital of Pd: this interaction has a greater overlap from I_2 in axial position (Scheme 24, Pd–I–I = 175.5°). As an electron-donating ligand, I_2 interacts with the empty $d_{x^2-y^2}$ orbital of Pd: this orbital interaction is maximized when I_2 coordinates to an equatorial position of the d^8 -Pd in a bent conformation (Scheme 23, Pd–I–I = 103.6°).⁵⁴



Scheme 24. Catalyzed C–H iodination with I_2 as oxidant following a Pd(II)/Pd(II) redox-neutral pathway.

I_2 as acceptor (EC) is energetically favored over I_2 as donor (OA), the barrier to their interconversion being $5.5 \text{ kcal}\cdot\text{mol}^{-1}$. In the Pd(II)/Pd(IV) redox pathway the rate-limiting barrier of the two-electron oxidation by I_2 was $14.7 \text{ kcal}\cdot\text{mol}^{-1}$ (at the I–I oxidative addition transition state), C–I reductive elimination occurs with a 10.6 kcal/mol barrier, and the overall C–H iodination step was exergonic by 18.4 kcal/mol leading to stable Pd(II) complex **d23** (Scheme 23).⁵⁴

Alternatively, the Pd(II)/Pd(II) redox-neutral pathway proceeds by I–I electrophilic attack on the Pd–C bond (Scheme 24). The terminal iodide is expelled and the proximal iodide (I1) is engaged “outer sphere” in bonding with the Pd and C centers. The calculated free energy barrier for the monomeric active catalyst is only $8.3 \text{ kcal}\cdot\text{mol}^{-1}$. This is significantly smaller than the energy required for (i) C–H activation ($14.3 \text{ kcal}\cdot\text{mol}^{-1}$) and (ii) iodination

MICROREVIEW

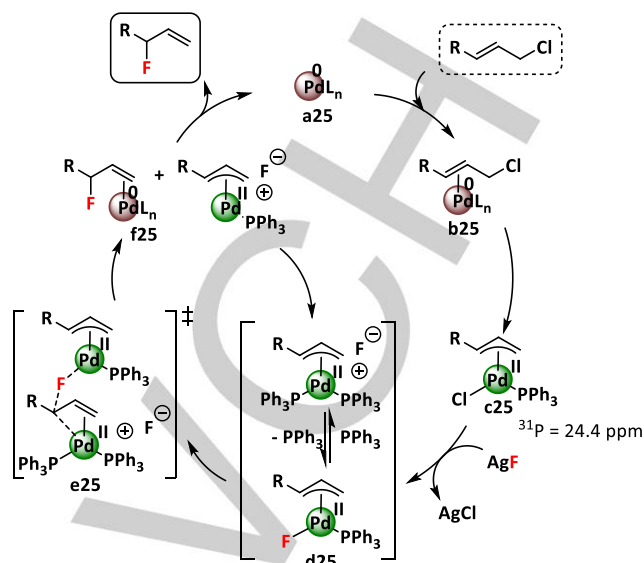
through the Pd(II)/Pd(IV) pathway (14.7 kcal.mol⁻¹). This EC step was calculated to be exergonic by 2.1 kcal.mol⁻¹, and the resulting intermediate **d24** presumably easily rearrange to thermodynamically more stable Pd(II) complex **d23** (Scheme 24).⁵⁴ Here again the calculated EC barrier at the corresponding dimeric transition states are 0.9 to 3.7 kcal.mol⁻¹ smaller than for the monomeric case, indicating that the Pd(II)–Pd(II) dimer would facilitate the electrophilic cleavage step. However, a second EC at the second palladium would provide a higher barrier (10.1 kcal.mol⁻¹) than the first one, still rather low.⁵⁴

As illustrated in Schemes 23 and 24, OA and EC stoichiometric pathways from monomeric Pd(OAc)₂ **a23** lead to the same IPd(OAc) complex, **d23** which could act as an active species for a second C–H iodination reaction. The calculated C–H activation, I–I oxidative addition, and I₂ electrophilic cleavage barriers are 14.7, 13.1, and 11.8 kcal/mol, respectively, from monomeric IPd(OAc) **d23**. Comparison of these energy values with those reported for Pd(OAc)₂ and IPd(OAc) active species proceed via comparable energy barriers. Thus, both the EC Pd(II)/Pd(II) redox-neutral and OA Pd(II)/Pd(IV) pathways will lead after two catalyst turnovers to the unreactive product PdI₂. Therefore, regeneration of Pd(OAc)₂ or IPd(OAc) from PdI₂ with CsOAc is necessary for catalyst turnover, as experimentally uncovered before.⁵³ Overall, Musaev, Yu and their co-workers have shown for C–H iodination that: (i) both monomeric and dimeric Pd(II) species can act as an active catalyst in the electrophilic C–H iodination process, (ii) the rate-determining step of this overall stoichiometric C–H iodination reaction is the CMD C–H bond activation, and (iii) the iodination of the C–H bond preferentially occurs via the EC mechanism regardless of monomeric or dimeric active species involvement. Even though the so-called OA pathway was computed to be less likely than the “outer sphere” EC pathway, the calculated OA barriers are not too high, which suggests the general feasibility of both pathways. In this theoretical study the authors investigated a series of substrates with commonly employed directing groups. For all studied C(sp²)–H substrates the EC iodination pathway is more favorable than the oxidative addition pathway, but increasing the DG donor ability increases the electrophilic iodination barrier, and reduces the I–I oxidative addition barrier.⁵⁴ These trends for C(sp²)–H substrates also hold for the C(sp³)–H substrates. However, the calculated OA and EC barriers are significantly higher for the C(sp³)–H substrates, and consequently for all studied C(sp³)–H only the weakest DGs would proceed via the EC pathway. Thus, an oxazoline DG in substrates was predicted to promote the formation of a Pd(IV) intermediate for C(sp³)–H iodination with an EC pathway disfavored by 11.1 kcal.mol⁻¹.

Finally, the impact of the nature of the electrophile on the feasibility of the reported mechanisms of the C(sp²)–H bond halogenation has been examined. Halogen oxidants with 2σ* orbital (involved in the linear coordination of the electrophile to Pd center and the EC transition state) close to or below the energy level of that for I₂ can be effective electrophiles for the C(sp²)–H functionalization. One such electrophile is molecular bromine Br₂ (this is not the case for Cl₂, and NIS) and accordingly stoichiometric C(sp²)–H bromination using Pd(OAc)₂ and Br₂ confirmed these computational predictions.⁵⁴

Concerning C–F bond formation catalyzed by palladium, Doyle group reported the generation of a palladium fluoride **d25**

necessary to achieve selective C–F bond formation via “outer-sphere” nucleophilic attack (Scheme 25).⁵⁵

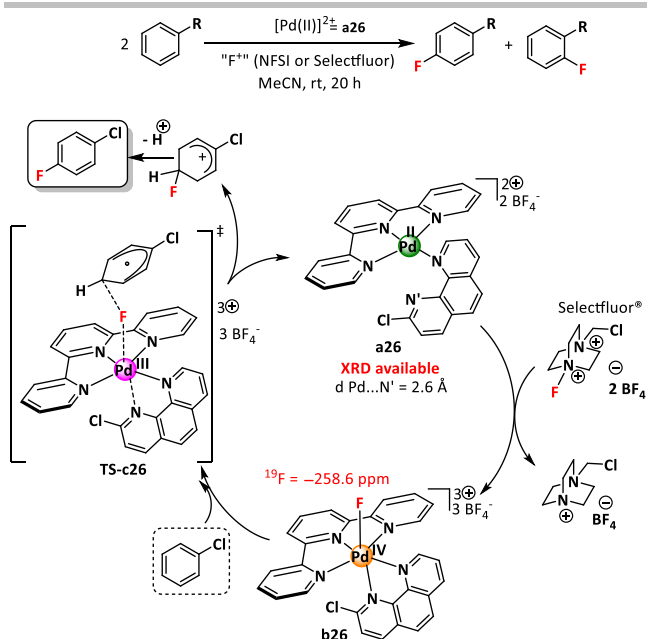


Scheme 25. “Outer-sphere” Pd-catalyzed nucleophilic allyl fluorination

Electrophilic fluorination catalyzed by ruthenium following an “outer sphere” mechanism has been also postulated by Lynam and Slaterry groups for the formation of alkenyl and alkyl C–F bonds in the coordination sphere of ruthenium organometallic complexes.⁵⁶

Most recently, Ritter group reported a so-called palladium-catalyzed electrophilic aromatic C–H fluorination (Scheme 26, top) somewhat related to the above-described “outer sphere” illustrative examples.⁵⁷ This reaction can be viewed as a breakthrough in direct electrophilic aromatic substitution (S_EAr) using “F⁺”, fluorine being –out of the four common halogens– the only one not amenable to typical S_EAr. The conventional approach for direct arene C–H electrophilic functionalization in the absence of a coordinating directing group requires multiple equivalents of the arene substrate to promote C–H metalation. Instead, Ritter group designed a highly reactive Pd(II) cationic precatalyst bearing ancillary ligands in an adequate geometry that favors its oxidation into high-valent metal-fluoride intermediate before any interaction with the arene substrate. The resulting reactive tricationic Pd(IV) is electrophilic at fluorine and capable of oxidative fluorine transfer to a wide scope of functionalized arenes. Electron-rich and electron-deficient arenes were thus coupled without DG groups, generally giving a balanced mixture of *para*- and *ortho*-fluorinated isomers.

MICROREVIEW



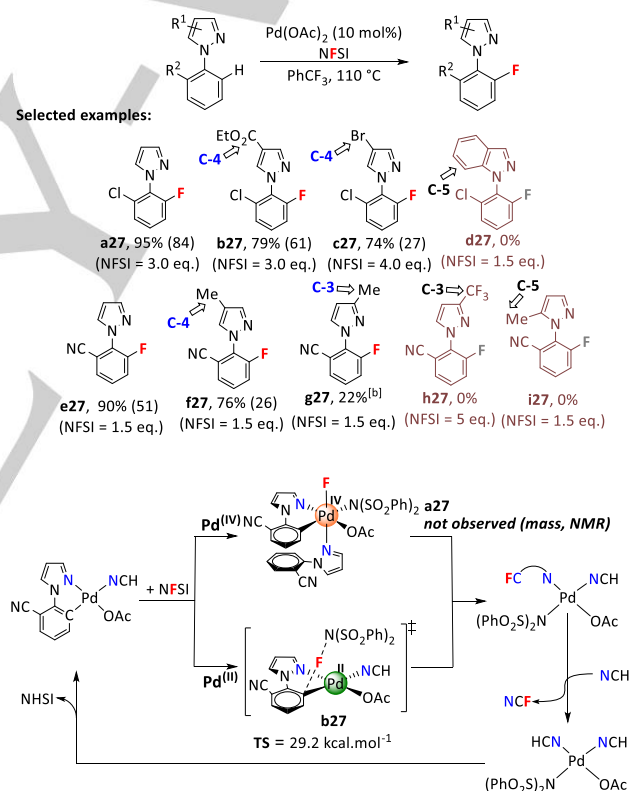
Scheme 26. Catalytic cycle proposed for palladium-catalyzed electrophilic aromatic C–H fluorination.

DFT calculations have shown that the oxidation of doubly cationic **a26** (Scheme 26, bottom) is promoted by a destabilizing interaction between the lone pair of the apical donor atom and the filled d_{z^2} orbital on Pd(II). X-ray diffraction corroborates the apical interaction: $d_{Pd...N'} = 2.6 \text{ \AA}$, which is 1.2 \AA shorter than the sum of the van der Waals radii of palladium and nitrogen. In the catalysis of aromatic oxidation reactions **a26** would first form Pd(IV)–F intermediate **b26**. The activated Pd(IV)–F electrophile **b26** would therefore be capable of electrophilic fluorination of weakly nucleophilic arenes that cannot be fluorinated directly by Selectfluor and NFSI. A DFT analysis of the aryl fluorination reaction suggests a mechanism that is accessible to Pd(IV)–F but not to Selectfluor or NFSI. Fluorination mechanism proceeds through a single transition state via fluoride-coupled electron transfer (**TS-c26**, Scheme 26). Conversely, Selectfluor fluorinated only electron-rich arenes such as anisole. DFT calculations suggested that tricationic **b26** has a higher potential of single-electron reduction than that of Selectfluor, although both compounds have a similar thermodynamic driving force for electrophilic fluorination. The transition state **TS-c26** leading to fluorination chlorobenzene shows high spin-density on the palladium as well as on the aryl carbon atoms. This transition state is thus appropriately described as a singlet diradical. According to the authors “two subsequent fluoride-coupled electron transfers occur asynchronously as the reaction proceeds through a single transition state”. This proposal is echoing that previously reported by the Ritter group for the fluorination of enamines and organometallic reagents with an isolated Pd(IV)–F intermediate.⁵⁸

The calculated energy barrier for this electrophilic fluorination is $21.8 \text{ kcal.mol}^{-1}$, which is consistent with the reaction conditions of time and temperature. Stoichiometric treatment of **a26** with XeF_2 in the presence of LiBF_4 produced a ^{19}F NMR signal attributable to **b26** at $\delta = -258.6$. However, the complex formed is reduced to **a26** in acetonitrile (even in the absence of substrate) which did not allow its isolation. Treatment of **a26** with Selectfluor ($-40 \text{ }^\circ\text{C}$ to $25 \text{ }^\circ\text{C}$) resulted in the desired reduction of Selectfluor, but did

not allow to observe any ^{19}F NMR signal that may be attributed to a Pd(IV)–F species. According to the authors, this occurs because **b26** is reduced faster than it is formed and does not accumulate in observable quantities. However, an analogous complex was formed in which 2-Cl-phen is replaced with unsubstituted phenanthroline (phen) which was treated with Selectfluor in acetonitrile at room temperature and then allowed to stand at $-35 \text{ }^\circ\text{C}$, a Pd(IV)–F complex ($^{19}\text{F} = -259.5 \text{ ppm}$) and isolated in 73% yield. This complex was sufficiently stable at low temperature to enable characterization and reactivity studies. Its higher stability was understood to result from the greater electron-donating ability of phen relative to that of 2-Cl-phen. Overall, the reactive dicationic/tricationic palladium catalysts provide a new access for arenes fluorination, in the absence of directing groups, via an “outer sphere” fluoride-coupled electron-transfer mechanism that is not accessible to electrophilic fluorinating reagents such as Selectfluor.

In 2015, Roger, Fleurat-Lessard and Hierso reported a general protocol for palladium-catalyzed C–H mono- and difluorination of highly substituted arylpyrazoles (Scheme 27, top).⁵⁹



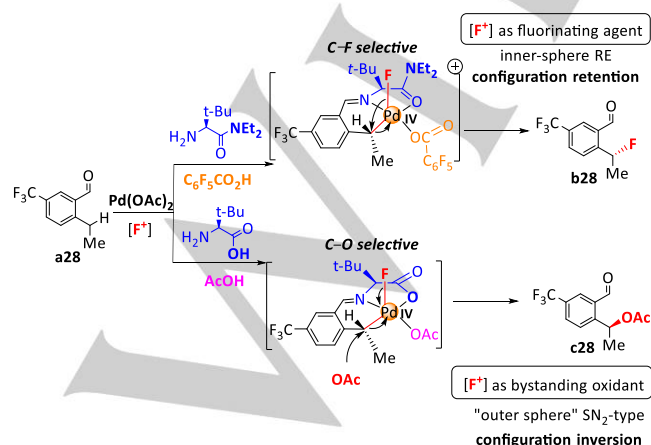
Scheme 27. Pd-catalyzed arylpyrazoles fluorination with alternative “outer sphere” NFSI attack.

The authors showed for the first time the influence of highly substituted directing groups on the course of palladium-catalyzed fluorination by NFSI, where steric substituent effects have a marked influence which was studied by calculations (details in section 5).⁵⁹ Substituents on the directing pyrazole unit have a dramatic influence on the reaction, rendering it generally more difficult. Nevertheless, C-4 substituted pyrazole units with electron-donating and electron-withdrawing functions such as ester (**b27**), bromide (**c27**) and methyl (**f27**) are tolerated (Scheme 27). Conversely, substitution of the pyrazole group at C-5 (**d27**, **i27**) inhibited fluorination, while contrasting results were

MICROREVIEW

obtained with C-3 substituted pyrazoles since an electron-withdrawing substituent trifluoromethyl fully inhibited fluorination (**h27**) while a donating methyl group allowed a modest conversion of 22% in **g27**. In the course of preliminary DFT modelling studies an alternative pathway to classical [Pd(II)/Pd(IV)] emerged that involved an "outer sphere" direct fluorination in which the metal center remains Pd(II) (Scheme 27, bottom). The barrier for this reaction was found at 29.2 kcal.mol⁻¹, which is not prohibitively high to consider this mechanism. This proposal was unusual but was consistent with the experimental issues related to the fairly high concentration of NFSI required (1.5-5.0 equiv), and as such may be further considered in the coming studies, as it has been done previously by Musaev and Yu for Pd-catalyzed electrophilic iodination.

Most recently, Yu group reported that controlling Pd(IV) reductive elimination pathways make feasible Pd(II)-catalyzed enantioselective *ortho*-C(sp³)-H fluorination of benzaldehydes (**a28**, Scheme 28) using a chiral transient directing group strategy.⁶⁰ A competition in chemoselectivity of a C(sp³)-F and C(sp³)-O bond-forming processes was observed, both with high stereoselectivity. Stereochemical analysis revealed that while C(sp³)-F formation proceeds via an inner-sphere pathway with retention of configuration (**b28**), the competing C(sp³)-O formation (**c28**) occurs through an "outer sphere" SN₂-type mechanism. The absolute stereochemistry of both **b28** and **c28** were identified by X-ray crystallography. The opposite absolute configuration of these two products was confirmed, indicating the involvement of two distinct reaction pathways. The configuration of **b28** is consistent with fluorination proceeding through a classic inner-sphere reductive elimination process with retention of stereochemistry, while **c28** is formed through an SN₂-type mechanism to achieve inversion of stereochemistry. The switch from neutral to cationic Pd(IV) not only reduces the energy level of σ*(Pd-C), which would accelerate all reductive elimination pathways, but also affects Pd-F bonding. Conversely, an *amino-acid-type* transient directing group will lead to a neutral, five-coordinate Pd(IV) intermediate that renders the desired C(sp³)-F reductive elimination slower than competing pathways (here "outer sphere" C(sp³)-O formation. Thus, the choice of anionic or neutral transient directing groups favors the formation of neutral or cationic Pd(IV) intermediates and offers an effective method for controlling reductive elimination pathways. The use of a *bulky amino amide* transient directing group was critical in achieving high enantioselectivity and promoting C-F reductive elimination.



Scheme 28. Chemoselective asymmetric C(sp³)-F and C(sp³)-O bond-forming processes.

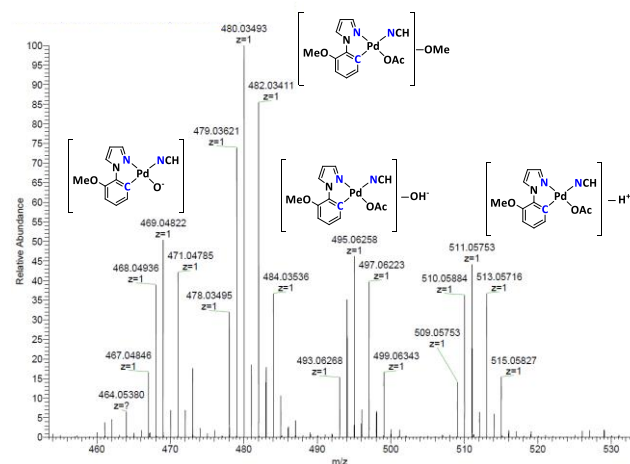
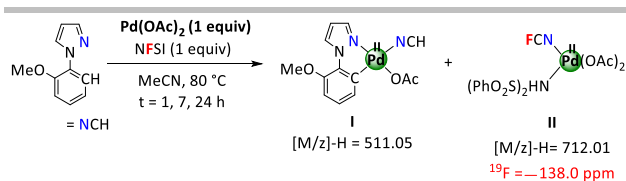
This set of selected "outer sphere" processes is a pertinent illustration of the intricate alternative mechanisms which have been identified recently for electrophilic fluorination and related halogenation reactions.

5. Selectivity effects in C-H fluorination related to palladacycles formation

Besides chemoselectivity issues between C-F formation and a number of competing C-X (X = O, N, C, etc.) bond formation (evoked in the previous sections, when "F⁺" play the role of bystanding oxidant in processes where reductive elimination for C-F is disfavored) interesting regioselectivity effects at C-H have been recently reported. Competition between mono and difluorination at free *ortho*-positions has been early on recognized but was generally poorly addressed.^{22b,33a} For instance, Yu group tried to avoid the difficult separation of the mono- and difluorinated products in *sp*²-C fluorination of *N*-benzylamine derivatives and *N*-arylbenzamides (Scheme 11). They attempted to achieve monoselectivity with benzylamine trifluoramide. While difluorinated product is obtained in 68% yield (~4% monofluorinated), the best yield of monofluorinated product was 41% (~7% difluorinated) when the reaction was performed using DMF instead of NMP.³³

In 2013, Xu group reported a [Pd(OAc)₂-NFSI-TFA] system for selective *ortho*-monofluorination of 2-phenylquinoxalines (Scheme 8).³⁰ Later, studies from Roger, Fleurat-Lessard and Hierso, on related aryl pyrazoles,⁵⁹ indicated that the issue of *N*-directed selective monofluorination of non-*ortho*-substituted arenes by adding a TFA promoter in the presence of CH₃NO₂ or NO₃ was due to a kinetic effect which increases the gap existing between the rates of monofluorination and subsequent difluorination reactions. However, mechanistic studies establishing the general course of *ortho*-difluorination with regards to *ortho*-monofluorination that could give a better knowledge for mastering monofluorination selectivity are still desirable. In their studies (Scheme 27), Roger and coworkers observed that C-4 substituents on the directing pyrazole unit were tolerated while substitution of the pyrazole group at C-5 and C-3 have a dramatic inhibiting influence on fluorination.⁵⁹ The mass spectrometry analysis of the stoichiometric reaction indicated the formation of monomeric palladium species with a fragmentation exemplified in Scheme 29 (bottom). These results contrasted with the studies reported by Xu et al.³⁰ that used related quinoxalines and oximes as *N*-directing ligands, since no isotopic mass *m/z* above 600 was detected with pyrazole substrates (see section 2.3). The signature of monomeric palladium complex **I** is clearly identified (isotopic distribution: Pd104 11%, Pd105 22%, Pd10627%, Pd108 26%, Pd110 11%). The palladium signature for dimer compounds is naturally very different but has typical isotopic mass distribution that should be clearly identified in any case. The resting state nature of this complex **I** was supported by the mass spectra obtained after 1 h, 7 h and 24 h of reaction with after this time the additional presence of complex **II** (*m/z* = 712.0, ¹⁹F = -138 ppm) incorporating a fluorinated pyrazole ligand (Scheme 29, top).

MICROREVIEW



Scheme 29. Mass analysis of arylpyrazole fluorination conducted under stoichiometric conditions.

Based on these monomeric palladacycles, the authors considered the effect of substituents on pyrazoles directing groups, and focused their calculations on the barrier for formation of fluorinated molecules **e27**–**i27** (Scheme 27) via palladacycles of the type of **I** (Scheme 29).⁵⁹ They compared the formation energy of the corresponding palladacycles for each fluorinated compound, showing that compared to **e27** formation which was obtained from pristine pyrazole DG, up to 8.4 kcal.mol⁻¹ is required for the formation of palladacycles **i27** and **h27**. This was representative of intra-ligand and inter-ligands steric interactions, respectively, which are at play in key intermediates and transition states. This was supported by the mapping of Non-Covalent Interaction (NCI) in such palladacycles (Figure 3), more important for **I-i27** and **I-h27**.

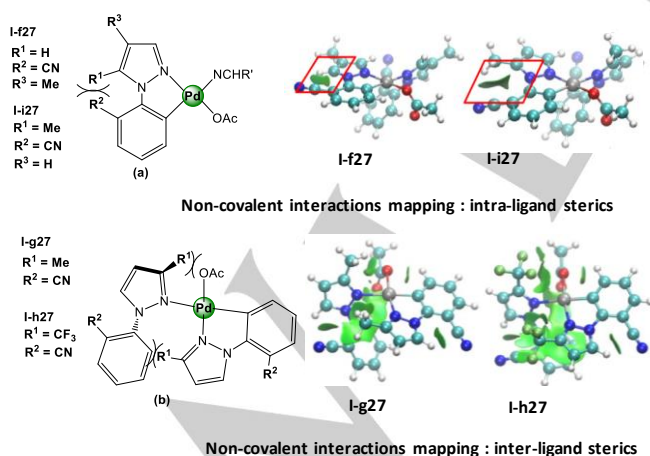
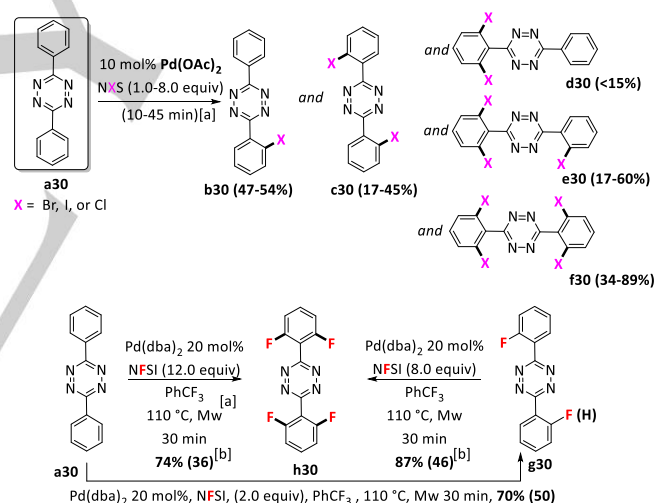


Figure 3. Non-Covalent Interaction (NCI) plots: the extent of green areas specifies the degree of steric interactions (H atoms in white, C pale blue, O red, N blue, F green, Pd grey). In **(a)** intramolecular NCI interactions are shown inside the red box (top). See Scheme 27 for fluorination conversion yields, *i.e.* **i27** = 76%, **i27** = 0% and **g27** = 22%, **h27** = 0%.

NCI shows for palladacycle **I-i27** intramolecular steric hindrance between the 5-Me-pyrazole and the phenyl moiety, also illustrated by the strong deviation from planarity between the two arene

cycles. In **I-h27** (or **I-g27**) the 3-CF₃ (or 3-Me) group creates an inter-ligands steric hindrance with the other pyrazole entity and OAc ligand (Figure 3). The 3-CF₃ group also withdraws electrons of the palladium-bonded nitrogen atom. Both effects contribute to destabilize the Pd(II) intermediates and are assumed to be major factors hampering the fluorination to proceed.

The Hierso group also introduced recently the use of diphenyl-1,2,4,5-tetrazine (*s*-tetrazine) as DG compatible with palladium-catalyzed electrophilic halogenation and fluorination (Scheme 30).⁶¹ C–H activation reaction is a challenging reaction for substituted tetrazines such as 3,6-diphenyl-1,2,4,5-tetrazine **a30** since this reactive nitrogen-rich heterocycle could be reduced and decomposed in the presence of metal. Additionally, the selectivity in C–H is affected by the presence of up to four sp²C–H bonds in *ortho*-position of the heteroaromatic ring for each nitrogen atom. Under mild conditions, palladium *N*-directed *ortho*-C–H activation of tetrazines allowed the introduction of various functions forming C–heteroatom bonds: C–X (X = I, Br, Cl, and F) and C–O. Selective electrophilic mono- and poly-*ortho*-functionalization of tetrazines was developed: mono-, di-, tri- and tetra-halogenation conditions were reported (Scheme 30, top). Microwave irradiation was optimized to afford C–F fluorinated *s*-aryltetrazines with satisfactory selectivity in only 10 min (Scheme 30, bottom). This work provided a practical entry for accessing *ortho*-substituted aryltetrazine derivatives that are not reachable by Pinner hydrazine condensation.⁶¹



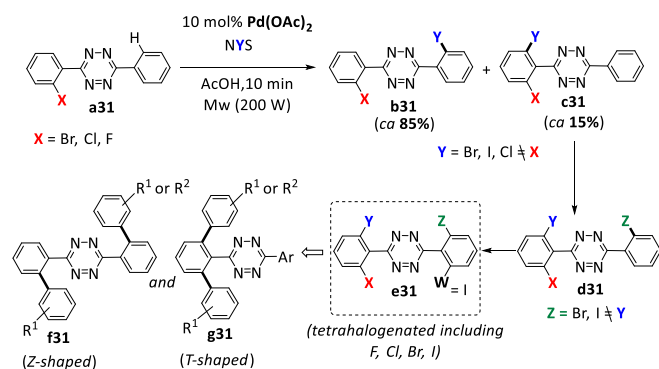
Scheme 30. Palladium-catalyzed polyhalogenation of *s*-aryltetrazines and di- and tetrafluorination. ^[a]Fast rates are promoted by microwave heating MW. ^[b]Isolated yields in brackets (*pure fluorinated products are challenging to isolate, and isolated yields are sometimes lacking in reports on C–H fluorination*).

The functionalization of **a30** with a variety of functions was achieved by tuning the protocols: monoiodination employed *N*-iodosuccinimide (NIS), chlorination used *N*-chlorosuccinimide (NCS) and acetoxylation used PhI(OAc)₂. Various C–H polyhalogenation reactions were also achieved, and for instance *o*-tetrafluoroaryltetrazine **h30** was obtained in very fast reactions promoted by microwave heating.⁶¹ The difluorinated **g30** (Scheme 30, bottom) was found to improve the reaction rate (2.13 times faster) of electron-deficient diene tetrazines coupling with electron-rich dienophiles to form a Diels–Alder adduct (*inverse electron-demand Diels–Alder reaction, iEDDA*). Fast reaction rates in fluorination and bioconjugation of aryltetrazines is

MICROREVIEW

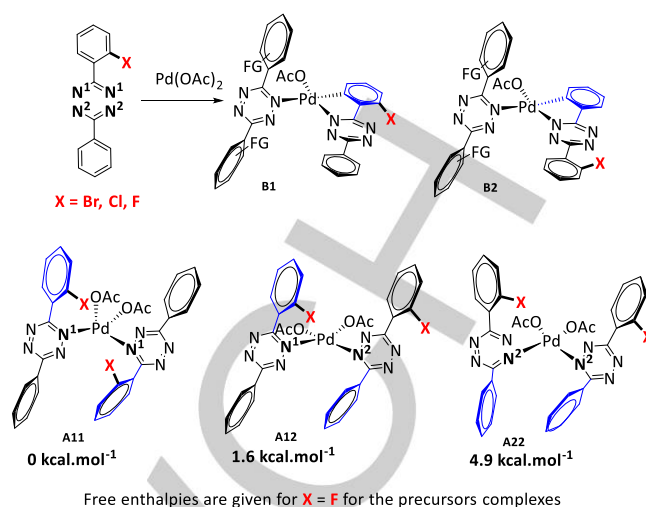
especially relevant in the perspective of further extension to [^{18}F] radiochemistry.⁶¹

In a follow-up, Roger and coworkers achieved a sequence of two or three selective halogenation reactions from **b30** and **c30**, in a specific order, to produce unsymmetrical polysubstituted reactive aryl halides (such as **b31–e31**), which were then used for the controlled synthesis of new biphenyls and unprecedented polyaromatic *s*-aryltetrazines such as *Z-shaped* **f31** and *T-shaped* **g31** (Scheme 31).⁶²



Scheme 31. Stepwise building of chemically differentiated tetrazines by selective C–H halogenation.

In these C–H halogenation sequences, single halogenation of monohalogenated *s*-aryltetrazines proceeded preferentially on the unsubstituted aryl moiety whatever the halide function present on the other aryl (Br, Cl or F, for **a31**) giving systematically a selectivity ca. 85% of **b31** and 15% of **c31**. To mechanistically clarify the origin of this selectivity the authors studied by DFT calculations the C–H functionalization focused at the formation of *N*-containing palladacycles as decisive intermediates in the process. The final selectivity observed was attributed to the concurrent formation of the intermediates **B1** and **B2** (Figure 4). Bis(acetato) Pd(II) complexes **A11**, **A12** and **A22** are pertinent precursors for the formation of **B1** and **B2**. **A11** is the most stable isomer, yet the isomerization barrier is fairly low (20.4 kcal.mol⁻¹) and thus the three isomers should co-exist in the reaction. The free enthalpy profiles were computed for the formation of palladacycles **B1** and **B2** from complexes **A** by C–H activation in a concerted metalation-deprotonation mechanism (CMD) assisted by AcOH. Free energies and geometries for the main TS were computed (Figure 5) for X = Br, Cl and F. DFT showed lower energy barriers for the C–H activation on the unsubstituted aryl moieties (**B2** formation) with transition structure **TS2** energies ranging from 31.7 kcal.mol⁻¹ (X = Cl) to 32.7 kcal.mol⁻¹ (X = Br). Halogenated aryl undergoes C–H activation with higher energy, **TS1** ranging from 32.0 kcal.mol⁻¹ (X = Cl) to 34.5 kcal.mol⁻¹ (X = Br). This trend was shared by all halogenated intermediates.



Electron-withdrawing substituents (halogen) already present on the targeted aryl group before halogenation increase the activation barrier to form the intermediate palladacycle. Thus, at elevated reaction temperature the halogenation of unsubstituted aryl moiety would be kinetically favored (**b31** preferred over **c31**).

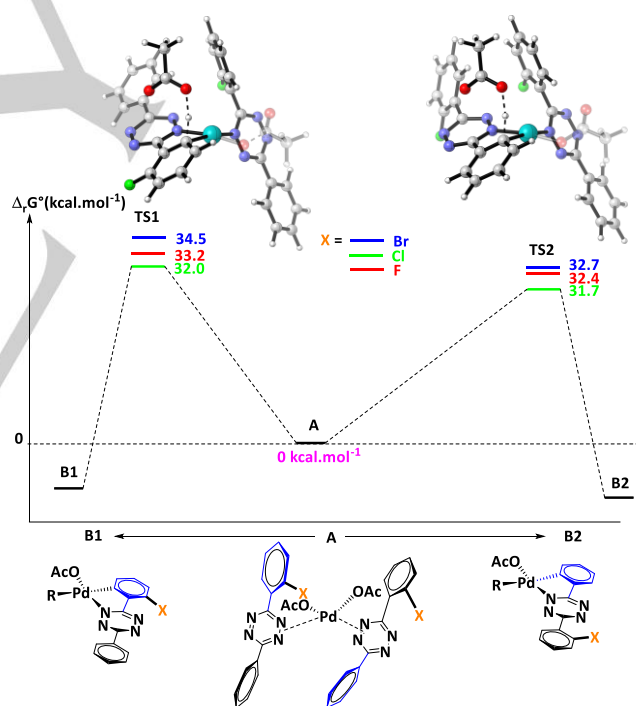


Figure 5. Free enthalpy profiles for C–H activation of *s*-aryltetrazines to form the intermediate palladacycle by CMD mechanism.

Under such kinetic control the selectivity ratio calculated using computed activation free energies were found to be 84:16 (X = F), 77:23 (X = Cl), 96:4 (X = Br), globally reproducing satisfactorily the experimental results.

The studies conducted on the selectivity of C–H functionalization in the presence of DGs which are already substituted are pertinent since the influence of elaborate substituted DGs on the course of palladium-promoted fluorination/halogenation received to date only limited attention.

MICROREVIEW

Yet, this question has a crucial synthetic utility to apply the methodologies beyond simple substrates and democratize it for total synthesis, or the synthesis of sophisticated pharmaceuticals. The steric influence of functionalized pyrazoles in arylpyrazoles, and the electronic influence of functionalized arenes in aryltetrazines were elucidated in relation with the stability and barrier to form of pertinent monomeric palladacycles. In this context, a small difference below 5.0 kcal.mol⁻¹ has clearly a dramatic effect for C–H selectivity, sometimes even hampering the reaction to proceed at reasonable temperature. This knowledge would certainly stimulate further reasoned modification of DGs towards steric and electronic more favorable factors.

6. Summary and outlook

While *N*-directed *ortho*-C–H bond electrophilic fluorination and related halogenation reactions based on palladium oxidation chemistry is a still young research topic, the recent years have experienced remarkable progress in the mechanistic understanding of selective functionalization of sp²-C–H and sp³-C–H bonds. Clearly, a high dependence in the reaction conditions has been demonstrated by the various studies. Changes in mechanistic pathways are expected as a function of the directing groups (distinguished as strongly or weakly coordinating), the solvents (distinguished as polar or apolar), the various oxidant (bystanding or reacting), the additives (acidic or basic, organic, inorganic), the steric/electronic modifications at substrates and directing groups. Stoichiometric approaches had the virtue to evidence that all formal oxidation state of palladium Pd(0), Pd(II), Pd(III) and Pd(IV) can be reached in processes for which mononuclear and dinuclear species can be involved (as possibly connected species –depending also on the concentration, additives and temperature reactions–). Such studies, sometimes supported by theoretical DFT computation, have evidenced the role of often demanding reductive elimination from Pd(IV) –which again can be facilitated or not by the nature of DGs–. From a catalytic perspective, while direct linking with stoichiometric evidences is not straightforward, detailed thorough kinetic studies have also driven progress in understanding, even if puzzling induction periods and rather sophisticated rate laws have been evidenced. Further progress is expected in the understanding of difluorination catalytic laws (and more generally in multiple halogenation reactions) and on mastering the selectivity trends in various C–H halogenations.

These fairly recent mechanistic works have been accompanied with impressive synthetic breakthroughs like the design of palladium dicationic complexes for electrophilic fluorination of arenes without DGs and excess reagent. Electrophilic fluorination reactions at room temperature in the presence of nitrate, or the smart control of stereoselectivity with transient chiral weakly bonding DGs also constituted great advances. Finally, the openings to new pertinent substrates like reactive bioconjugable tetrazines elegantly using multiple nitrogen atoms to devise manifold selective C–H functionalization are expected to be useful in the future.

Acknowledgements

This work was supported by the CNRS, Université de Bourgogne (MESR PhD grant for CT), Conseil Régional de Bourgogne through the Plan d' Actions Régional pour l'Innovation (PARI projects 3MIM and CDEA) and the Fonds Européen de Développement Régional (FEDER). We are thankful for specific support from the Institut Universitaire de France IUF (JCH) and CNRS mobility (PFL). J. R. benefited from a ISITE-COMUE BFC support (UB180013.MUB.IS-SmartTZ) for developing catalytic halogenation and fluorination.

Keywords: catalysis • fluorination • C–H halogenation • palladium • mechanisms • X-ray structures • kinetics • NMR •

- [1] F. H. Vaillancourt, E. Yeh, D. A. Vosburg, S. Garneau-Tsodikova, C. T. Walsh, *Chem. Rev.* **2006**, *106*, 3364–3378.
- [2] a) P. O. Wennberg, R. C. Cohen, R. M. Stimpfle, J. P. Koplów, J. G. Anderson, J. G.; R. J. Salawitch, D. W. Fahey, E. L. Woodbridge, E. R. Keim, R. S. Gao, C. R. Webster, R. D. May, D. W. Toohey, L. M. Avallone, M. H. Proffitt, M. Loewenstein, J. R. Podolske, K. R. Chan, S. C. Wofsy, *Science* **1994**, *266*, 398–404; b) M. J. Molina, T. L. Tso, L. T. Molina, F. C. Y. Wang, *Science* **1987**, *238*, 1253–1257.
- [3] Natural combustion processes, such as volcanoes (and other geothermal events occurring in lakes, soils, salt mines, etc.) and forest or savannah fires, contribute measurable quantities of halogenated organic compounds to the environment, see for instance: E. J. Hoekstra, E. W. B.; de Leer, U. A. Th. Brinkman, *Environ. Sci. Technol.* **1998**, *32*, 3724–3729; A. Ruecker, P. Weigold, S. Behrens, M. Jochmann, J. Laaks, A. Kappler, *Environ. Sci. Technol.* **2014**, *48*, 9170–9178 and references therein.
- [4] A. Vigalok, *Chem.–Eur. J.* **2008**, *14*, 5102–5108.
- [5] J. M. Brown, V. Gouverneur, *Angew. Chem. Int. Ed.* **2009**, *48*, 8610–8614.
- [6] W. Liu, T. J. Groves, *Acc. Chem. Res.* **2015**, *48*, 1727–1735.
- [7] M. G. Campbell, T. Ritter, *Chem. Rev.* **2015**, *115*, 612–633.
- [8] D. A. Petrone, J. Ye, M. Lautens, *Chem. Rev.* **2016**, *116*, 8003–8104.
- [9] T. W. Lyons, M. S. Sanford, *Chem. Rev.* **2010**, *110*, 1147–1169.
- [10] a) D. Kalyani, A. R. Dick, W. Q. Anani, M. S. Sanford, *Tetrahedron* **2006**, *62*, 11483–11498; b) J. M. Racowski, M. S. Sanford, *Top. Organomet. Chem.* **2011**, *35*, 61–84; c) S. R. Neufeldt, M. S. Sanford, *Acc. Chem. Res.* **2012**, 936–946.
- [11] a) T. Furuya, A. S. Kamlet, T. Ritter, *Nature* **2011**, *473*, 470–477; b) T. Liang, C. N. Neumann, T. Ritter, *Angew. Chem. Int. Ed.* **2013**, *52*, 8214–8264.
- [12] a) X. Jiang, H. Liu, Z. Gu, *Asian J. Org. Chem.* **2012**, *1*, 16–24; b) C. Chen, X. Tong, *Org. Chem. Front.* **2014**, *1*, 439–446; c) A. Lin, C.B. Huehls, J. Yang, *Org. Chem. Front.* **2014**, *1*, 434–438.
- [13] A. Vigalok, *Acc. Chem. Res.* **2015**, *48*, 238–247.
- [14] K. M. Engle, T.-S. Mei, X. Wang, J.-Q. Yu, *Angew. Chem. Int. Ed.* **2011**, *50*, 1478–1491.
- [15] a) D. R. Fahey, *J. Chem. Soc., Chem. Commun.* **1970**, 417–417; b) D. R. Fahey, *J. Organomet. Chem.* **1971**, *27*, 283–292.
- [16] P. K. Byers, A. J. Canty, B. W. Skelton, A. H. White, *J. Chem. Soc., Chem. Commun.* **1986**, 1722–1724.
- [17] P. M. Henry, *J. Org. Chem.* **1971**, *36*, 1886–1890.
- [18] L. M. Stock, K.-T. Tse, L. J. Vorvick, S. A. Walstrum, *J. Org. Chem.* **1981**, *46*, 1757–1759.
- [19] T. Yoneyama, R. H. Crabtree, *J. Mol. Catal. A: Chem.* **1996**, *108*, 35–40.
- [20] A. R. Dick, K. L. Hull, M. S. Sanford, *J. Am. Chem. Soc.* **2004**, *126*, 2300–2301.
- [21] a) D. Kalyani, N. R. Deprez, L. V. Desai, M. S. Sanford, *J. Am. Chem. Soc.* **2005**, *127*, 7330–7331; b) K. L. Hull, E. L. Lanni, M. S. Sanford, *J. Am. Chem. Soc.* **2006**, *128*, 14047–14049.
- [22] a) D. Kalyani, A. R. Dick, W. Q. Anani, M. S. Sanford, *Org. Lett.* **2006**, *8*, 2523–2526; b) K. L. Hull, W. Q. Anani, M. S. Sanford, *J. Am. Chem. Soc.* **2006**, *128*, 7134–7135.

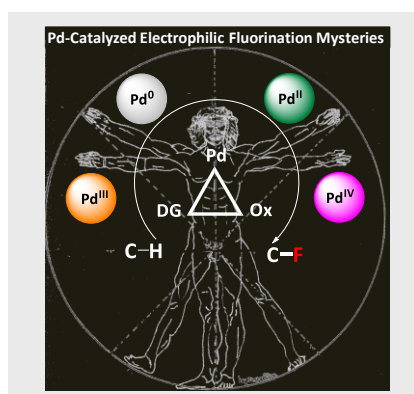
MICROREVIEW

- [23] a) T. Furuya, T. Ritter, *J. Am. Chem. Soc.* **2008**, *130*, 10060–10061; b) T. Furuya, D. Benitez, E. Tkatchouk, A. E. Strom, P. Tang, W. A. Goddard III, T. Ritter, *J. Am. Chem. Soc.* **2010**, *132*, 3793–3807; c) T. Furuya, D. Benitez, E. Tkatchouk, A. E. Strom, P. Tang, W. A. Goddard III, T. Ritter, *J. Am. Chem. Soc.* **2010**, *132*, 5922–5922.
- [24] A. W. Kaspi, A. Yahav-Levi, I. Goldberg, A. Vigalok, *Inorg. Chem.* **2008**, *47*, 5–7.
- [25] Other Trans-fluoride Pd(II) complexes are known with ^{19}F NMR ranging in 219.0 to 270.0 ppm, see: V. V. Grushin, W. J. Marshall, *J. Am. Chem. Soc.* **2009**, *131*, 918–919, and references therein.
- [26] a) W. J. Marshall, D. L. Thorn, V. V. Grushin, *Organometallics* **1998**, *17*, 5427–5430; b) N. A. Jasim, R. N. Perutz, A. C. Whitwood, T. Braun, J. Inzudu, B. Neumann, S. Rorhfeld, H.-G. Stammler, *Organometallics* **2004**, *23*, 6140–6149.
- [27] N. D. Ball, M. S. Sanford, *J. Am. Chem. Soc.* **2009**, *131*, 3796–3797.
- [28] J. M. Racowski, B. Gary, M. S. Sanford, *Angew. Chem. Int. Ed.* **2012**, *51*, 3414–3417.
- [29] J.-C. Hierso, *Chem. Rev.* **2014**, *114*, 4838–4867.
- [30] S.-J. Lou, D.-Q. Xu, A.-B. Xia, Y.-F. Wang, Y. Liu, X.-H. Du, Z.-Y. Xu, *Chem. Commun.* **2013**, *49*, 6218–6220.
- [31] S.-J. Lou, D.-Q. Xu, Z.-Y. Xu, *Angew. Chem. Int. Ed.* **2014**, *39*, 10330–10335.
- [32] Accordingly, we corrected herein the original proposal for the structure of intermediate **a10**.
- [33] a) X. Wang, T.-S. Mei, J.-Q. Yu, *J. Am. Chem. Soc.* **2009**, *131*, 7520–7521; b) K. S. L. Chan, M. Wasa, X. Wang, J.-Q. Yu, *Angew. Chem. Int. Ed.* **2011**, *50*, 9081–9084; c) J.-Q. Yu, US 2014/0018566 A1.
- [34] R.-Y. Zhu, K. Tanaka, G.-C. Li, J. He, H.-Y. Fu, S.-H. Li, J.-Q. Yu, *J. Am. Chem. Soc.* **2015**, *137*, 7067–7070.
- [35] Q. Zhang, X.-S. Yin, K. Chen, S.-Q. Zhang, B.-F. Shi, *J. Am. Chem. Soc.* **2015**, *137*, 8219–8226.
- [36] Q. Zhu, D. Ji, T. Liang, X. Wang, Y. Xu, *Org. Lett.* **2015**, *17*, 3798–3801.
- [37] S. Qiu, T. Xu, J. Zhou, Y. Guo, G. Liu, *J. Am. Chem. Soc.* **2010**, *132*, 2856–2857.
- [38] Pd–F species resonating as sharp singlets at –386.0 and –392.9 ppm resulting from Pd(II)-pyridine complexes decomposition have been reported by Grushin and Marshall, see ref. [25].
- [39] X.-Y. Chen, E. J. Sorensen, *J. Am. Chem. Soc.* **2018**, *140*, 2789–2792.
- [40] a) D. C. Powers, T. Ritter, *Nat. Chem.* **2009**, *1*, 302–309; b) M. G. Campbell, D. C. Powers, J. Raynaud, M. J. Graham, P. Xie, E. Lee T. Ritter, *Nat. Chem.* **2011**, *3*, 949–953.
- [41] N. R. Deprez, M. S. Sanford, *J. Am. Chem. Soc.* **2009**, *131*, 11234–12241.
- [42] Y. Ye, N. D. Ball, J. W. Kampf, M. S. Sanford, *J. Am. Chem. Soc.* **2010**, *132*, 14682–14687.
- [43] X. Wang, L. Truesdale, J.-Q. Yu, *J. Am. Chem. Soc.* **2010**, *132*, 3648–3649.
- [44] D. C. Powers, E. Lee, A. Ariafard, M. S. Sanford, B. F. Yates, A. J. Canty, T. Ritter, *J. Am. Chem. Soc.* **2012**, *134*, 12002–12009.
- [45] a) D. C. Powers, T. Ritter, *Acc. Chem. Res.* **2012**, *45*, 840–850; b) For a review of Pd(III) in synthesis and catalysis, including dinuclear Pd structure and chemistry, see: D. C. Powers, T. Ritter, *Top. Organomet. Chem.* **2011**, *35*, 129–156.
- [46] A. Ariafard, C. J. T. Hyland, A. J. Canty, M. Sharma, N. J. Brookes, B. F. Yates, *Inorg. Chem.* **2010**, *49*, 11249–11253.
- [47] F. A. Cotton, J. Gu, C. A. Murillo, D. J. Timmons, *J. Am. Chem. Soc.* **1998**, *120*, 13280–13281.
- [48] F. A. Cotton, M. Matusz, R. Poli, X. Feng, *J. Am. Chem. Soc.* **1988**, *110*, 1144–1154.
- [49] D. C. Powers, M. A. L. Geibel, J. E. M. N. Klein, T. Ritter, *J. Am. Chem. Soc.* **2009**, *131*, 17050–17051.
- [50] D. C. Powers, D. Benitez, E. Tkatchouk, W. A. Goddard III, T. Ritter, *J. Am. Chem. Soc.* **2010**, *132*, 14092–14103.
- [51] M. C. Nielsen, E. Lyngvi, F. Schoenebeck, *J. Am. Chem. Soc.* **2013**, *135*, 1978–1985.
- [52] B. E. Haines, J. F. Berry, J.-Q. Yu, D. G. Musaev, *ACS Catal.* **2016**, *6*, 829–839.
- [53] X.-C. Wang, Y. Hu, S. Bonacorsi, Y. Hong, R. Burrell, J.-Q. Yu, *J. Am. Chem. Soc.* **2013**, *135*, 10326–10329.
- [54] B. E. Haines, H. Xu, P. Verma, X.-C. Wang, J.-Q. Yu, D. G. Musaev, *J. Am. Chem. Soc.* **2015**, *137*, 9022–9031.
- [55] M. H. Katcher, P.-O. Norrby, A. G. Doyle, *Organometallics* **2014**, *33*, 2121–2133.
- [56] a) L. M. Milner, N. E. Pridmore, A. C. Whitwood, J. M. Lynam, J. M. Slattery, *J. Am. Chem. Soc.* **2015**, *137*, 10753–10759; (b) L. M. Milner, L. M. Hall, N. E. Pridmore, M. K. Skeats, A. C. Whitwood, J. M. Lynam, J. M. Slattery, *Dalton Trans.* **2016**, *45*, 1717–1726.
- [57] K. Yamamoto, J. Li, J. A. O. Garber, J. D. Rolfes, G. B. Boursalian, J. C. Borghs, C. Genicot, J. Jacq, M. van Gastel, F. Neese, T. Ritter, *Nature*, **2018**, *554*, 511–554.
- [58] J. R. Brandt, E. Lee, G. B. Boursalian, T. Ritter, *Chem. Sci.* **2014**, *5*, 169–179.
- [59] C. Testa, J. Roger, S. Scheib, P. Fleurat-Lessard, J.-C. Hierso, *Adv. Synth. Catal.* **2015**, *357*, 2913–2923.
- [60] H. Park, P. Verma, K. Hong, J.-Q. Yu, *Nat. Chem.* **2018**, *10*, 755–762.
- [61] C. Testa, E. Gigot, S. Genc, R. Decréau, J. Roger, J.-C. Hierso, *Angew. Chem. Int. Ed.* **2016**, *55*, 5555–5559.
- [62] C. D. Mboyi, C. Testa, S. Reeb, S. Genc, H. Cattey, P. Fleurat-Lessard, J. Roger, J.-C. Hierso, *ACS Catalysis* **2017**, *7*, 8493–8501.

Entry for the Table of Contents

MICROREVIEW

Selective C–H bond fluorination using palladium catalysis is a challenging reaction, and exciting mechanistic studies revealed some of its mysterious trends. Recent related synthetic advances are also available for the “Vitruvian” Chemists.



C–H Electrophilic Fluorination*

C. Testa, J. Roger,* Paul Fleurat-Lessard,* and Jean-Cyrille Hierso*

Page No. – Page No.

Palladium-Catalyzed C–H Bond Electrophilic Fluorination: Mechanistic Overview and Supporting Evidences

Automated References

- 1 F. H. Vaillancourt, E. Yeh, D. A. Vosburg, S. Garneau-Tsodikova, C. T. Walsh, *Chem. Rev.* 2006, 106, 3364–3378.
- 2 a) P. O. Wennberg, R. C. Cohen, R. M. Stimpfle, J. P. Koplrow, J. G. Anderson, J. G.; R. J. Salawitch, D. W. Fahey, E. L. Woodbridge, E. R. Keim, R. S. Gao, C. R. Webster, R. D. May, D. W. Toohy, L. M. Avallone, M. H. Proffitt, M. Loewenstein, J. R. Podolske, K. R. Chan, S. C. Wofsy, *Science* 1994, 266, 398–404; b) M. J. Molina, T. L. Tso, L. T. Molina, F. C. Y. Wang, *Science* 1987, 238, 1253–1257.
- 3 Natural combustion processes, such as volcanoes (and other geothermal events occurring in lakes, soils, salt mines, etc.) and forest or savannah fires, contribute measurable quantities of halogenated organic compounds to the environment, see for instance: E. J. Hoekstra, E. W. B.; de Leer, U. A. Th. Brinkman, *Environ. Sci. Technol.* 1998, 32, 3724–3729; A. Ruecker, P. Weigold, S. Behrens, M. Jochmann, J. Laaks, A. Kappler, *Environ. Sci. Technol.* 2014, 48, 9170–9178 and references therein.
- 4 A. Vignalok, *Chem.-Eur. J.* 2008, 14, 5102–5108.
- 5 J. M. Brown, V. Gouverneur, *Angew. Chem. Int. Ed.* 2009, 48, 8610–8614.
- 6 W. Liu, T. J. Groves, *Acc. Chem. Res.* 2015, 48, 1727–1735.
- 7 M. G. Campbell, T. Ritter, *Chem. Rev.* 2015, 115, 612–633.
- 8 D. A. Petrone, J. Ye, M. Lautens, *Chem. Rev.* 2016, 116, 8003–8104.
- 9 T. W. Lyons, M. S. Sanford, *Chem. Rev.* 2010, 110, 1147–1169.
- 10 a) D. Kalyani, A. R. Dick, W. Q. Anani, M. S. Sanford, *Tetrahedron* 2006, 62, 11483–11498; b) J. M. Racowski, M. S. Sanford, *Top. Organomet. Chem.* 2011, 35, 61–84; c) S. R. Neufeldt, M. S. Sanford *Acc. Chem. Res.* 2012, 936–946.
- 11 a) T. Furuya, A. S. Kamlet, T. Ritter, *Nature* 2011, 473, 470–477; b) T. Liang, C. N. Neumann, T. Ritter, *Angew. Chem. Int. Ed.* 2013, 52, 8214–8264.
- 12 a) X. Jiang, H. Liu, Z. Gu, *Asian J. Org. Chem.* 2012, 1, 16–24; b) C. Chen, X. Tong, *Org. Chem. Front.* 2014, 1, 439–446; c) A. Lin, C. B. Huehls, J. Yang, *Org. Chem. Front.* 2014, 1, 434–438.
- 13 A. Vignalok, *Acc. Chem. Res.* 2015, 48, 238–247.
- 14 K. M. Engle, T.-S. Mei, X. Wang, J.-Q. Yu, *Angew. Chem. Int. Ed.* 2011, 50, 1478–1491.
- 15 a) D. R. Fahey, *J. Chem. Soc., Chem. Commun.* 1970, 417–417; b) D. R. Fahey, *J. Organomet. Chem.* 1971, 27, 283–292.
- 16 P. K. Byers, A. J. Canty, B. W. Skelton, A. H. White, *J. Chem. Soc., Chem. Commun.* 1986, 1722–1724.
- 17 P. M. Henry, *J. Org. Chem.* 1971, 36, 1886–1890.
- 18 L. M. Stock, K.-T. Tse, L. J. Vorvick, S. A. Walstrum, *J. Org. Chem.* 1981, 46, 1757–1759.
- 19 T. Yoneyama, R. H. Crabtree, *J. Mol. Catal. A: Chem.* 1996, 108, 35–40.
- 20 A. R. Dick, K. L. Hull, M. S. Sanford, *J. Am. Chem. Soc.* 2004, 126, 2300–2301.
- 21 a) D. Kalyani, N. R. Deprez, L. V. Desai, M. S. Sanford, *J. Am. Chem. Soc.* 2005, 127, 7330–7331; b) K. L. Hull, E. L. Lanni, M. S. Sanford, *J. Am. Chem. Soc.* 2006, 128, 14047–14049.
- 22 a) D. Kalyani, A. R. Dick, W. Q. Anani, M. S. Sanford, *Org. Lett.* 2006, 8, 2523–2526; b) K. L. Hull, W. Q. Anani, M. S. Sanford, *J. Am. Chem. Soc.* 2006, 128, 7134–7135.
- 23 a) T. Furuya, T. Ritter, *J. Am. Chem. Soc.* 2008, 130, 10060–10061; b) T. Furuya, D. Benitez, E. Tkatchouk, A. E. Strom, P. Tang, W. A. Goddard III, T. Ritter, *J. Am. Chem. Soc.* 2010, 132, 5922–5922.
- 24 A. W. Kaspi, A. Yahav-Levi, I. Goldberg, A. Vignalok, *Inorg. Chem.* 2008, 47, 5–7.
- 25 Other Trans-fluoride Pd(II) complexes are known with ¹⁹F NMR ranging in 219.0 to 270.0 ppm, see: V. V. Grushin, W. J. Marshall, *J. Am. Chem. Soc.* 2009, 131, 918–919, and references therein.
- 26 a) W. J. Marshall, D. L. Thorn, V. V. Grushin, *Organometallics* 1998, 17, 5427–5430; b) N. A. Jasim, R. N. Perutz, A. C. Whitwood, T. Braun, J. Inzuda, B. Neumann, S. Rorhfeld, H.-G. Stammler, *Organometallics* 2004, 23, 6140–6149.
- 27 N. D. Ball, M. S. Sanford, *J. Am. Chem. Soc.* 2009, 131, 3796–3797.
- 28 J. M. Racowski, J.; B. Gary, M. S. Sanford, *Angew. Chem. Int. Ed.* 2012, 51, 3414–3417.
- 29 J.-C. Hierso, *Chem. Rev.* 2014, 114, 4838–4867.
- 30 S.-J. Lou, D.-Q. Xu, A.-B. Xia, Y.-F. Wang, Y. Liu, X.-H. Du, Z.-Y. Xu, *Chem. Commun.* 2013, 49, 6218–6220.
- 31 S.-J. Lou, D.-Q. Xu, Z.-Y. Xu, *Angew. Chem. Int. Ed.* 2014, 39, 10330–10335.
- 32 Accordingly, we corrected herein the original proposal for the structure of intermediate **a10**.
- 33 a) X. Wang, T.-S. Mei, J.-Q. Yu, *J. Am. Chem. Soc.* 2009, 131, 7520–7521; b) K. S. L. Chan, M. Wasa, X. Wang, J.-Q. Yu, *Angew. Chem. Int. Ed.* 2011, 50, 9081–9084; c) J.-Q. Yu, *US 2014/0018566 A1*.
- 34 R.-Y. Zhu, K. Tanaka, G.-C. Li, J. He, H.-Y. Fu, S.-H. Li, J.-Q. Yu, *J. Am. Chem. Soc.* 2015, 137, 7067–7070.
- 35 Q. Zhang, X.-S. Yin, K. Chen, S.-Q. Zhang, B.-F. Shi, *J. Am. Chem. Soc.* 2015, 137, 8219–8226.
- 36 Q. Zhu, D. Ji, T. Liang, X. Wang, Y. Xu, *Org. Lett.* 2015, 17, 3798–3801.
- 37 S. Qiu, T. Xu, J. Zhou, Y. Guo, G. Liu, *J. Am. Chem. Soc.* 2010, 132, 2856–2857.
- 38 Pd-F species resonating as sharp singlets at –386.0 and –392.9 ppm resulting from Pd(II)-pyridine complexes decomposition have been reported by Grushin and Marshall, see ref. 25.
- 39 X.-Y. Chen, E. J. Sorensen, *J. Am. Chem. Soc.* 2018, 140, 2789–2792.
- 40 a) D. C. Powers, T. Ritter, *Nat. Chem.* 2009, 1, 302–309; b) M. G. Campbell, D. C. Powers, J. Raynaud, M. J. Graham, P. Xie, E. Lee, T. Ritter, *Nat. Chem.* 2011, 3, 949–953.
- 41 N. R. Deprez, M. S. Sanford, *J. Am. Chem. Soc.* 2009, 131, 11234–11241.
- 42 Y. Ye, N. D. Ball, J. W. Kampf, M. S. Sanford, *J. Am. Chem. Soc.* 2010, 132, 14682–14687.
- 43 X. Wang, L. Truesdale, J.-Q. Yu, *J. Am. Chem. Soc.* 2010, 132, 3648–3649.
- 44 D. C. Powers, E. Lee, A. Ariafard, M. S. Sanford, B. F. Yates, A. J. Canty, T. Ritter, *J. Am. Chem. Soc.* 2012, 134, 12002–12009.
- 45 a) D. C. Powers, T. Ritter, *Acc. Chem. Res.* 2012, 45, 840–850; b) For a review of Pd(III) in synthesis and catalysis, including dinuclear Pd structure and chemistry, see: D. C. Powers, T. Ritter, *Top. Organomet. Chem.* 2011, 35, 129–156.
- 46 A. Ariafard, C. J. T. Hyland, A. J. Canty, M. Sharma, N. J. Brookes, B. F. Yates, *Inorg. Chem.* 2010, 49, 11249–11253.
- 47 F. A. Cotton, J. Gu, C. A. Murillo, D. J. Timmons, *J. Am. Chem. Soc.* 1998, 120, 13280–13281.
- 48 F. A. Cotton, M. Matusz, R. Poli, X. Feng, *J. Am. Chem. Soc.* 1988, 110, 1144–1154.
- 49 D. C. Powers, M. A. L. Geibel, J. E. M. N. Klein, T. Ritter, *J. Am. Chem. Soc.* 2009, 131, 17050–17051.
- 50 D. C. Powers, D. Benitez, E. Tkatchouk, W. A. Goddard III, T. Ritter, *J. Am. Chem. Soc.* 2010, 132, 14092–14103.
- 51 M. C. Nielsen, E. Lyngvi, F. Schoenebeck, *J. Am. Chem. Soc.* 2013, 135, 1978–1985.
- 52 B. E. Haines, J. F. Berry, J.-Q. Yu, D. G. Musaev, *ACS Catal.* 2016, 6, 829–839.
- 53 X.-C. Wang, Y. Hu, S. Bonacorsi, Y. Hong, R. Burrell, J.-Q. Yu, *J. Am. Chem. Soc.* 2013, 135, 10326–10329.
- 54 B. E. Haines, H. Xu, P. Verma, X.-C. Wang, J.-Q. Yu, D. G. Musaev, *J. Am. Chem. Soc.* 2015, 137, 9022–9031.
- 55 M. H. Katcher, P.-O. Norrby, A. G. Doyle, *Organometallics* 2014, 33, 2121–2133.
- 56 (a) L. M. Milner, N. E. Pridmore, A. C. Whitwood, J. M. Lynam, J. M. Slattery, *J. Am. Chem. Soc.* 2015, 137, 10753–10759; (b) L. M. Milner, L. M. Hall, N. E. Pridmore, M. K. Skeats, A. C. Whitwood, J. M. Lynam, J. M. Slattery, *Dalton Trans.* 2016, 45, 1717–1726.
- 57 K. Yamamoto, J. Li, J. A. O. Garber, J. D. Rolfes, G. B. Boursalian, J. C. Borghs, C. Genicot, J. Jacq, M. van Gastel, F. Neese, T. Ritter, *Nature*, 2018, 554, 511–514.
- 58 J. R. Brandt, E. Lee, G. B. Boursalian, T. Ritter, *Chem. Sci.* 2014, 5, 169–179.
- 59 C. Testa, J. Roger, S. Scheib, P. Fleurat-Lessard, J.-C. Hierso, *Adv. Synth. Catal.* 2015, 357, 2913–2923.
- 60 H. Park, P. Verma, K. Hong, J.-Q. Yu, *Nat. Chem.* 2018, 10, 755–762.
- 61 C. Testa, E. Gigot, S. Genc, R. Decréau, J. Roger, J.-C. Hierso, *Angew. Chem. Int. Ed.* 2016, 55, 5555–5559.
- 62 C. D. Mboyi, C. Testa, S. Reeb, S. Genc, H. Cattet, P. Fleurat-Lessard, J. Roger, J.-C. Hierso, *ACS Catalysis* 2017, 7, 8493–8501.